Flow Modeling and Simulation in Pipelines

Luis Fernando Gonçalves Pires, Claudio Veloso Barreto, and Angela Ourivio Nieckele

Contents

L. F. G. Pires · C. V. Barreto
SIMDUT (Pipeline Thermo-Hydraulic Simulation Group), PUC-Rio (Pontifical Catholic University of Rio de Janeiro), Rio de Janeiro, Brazil
e-mail: lpires@esp.puc-rio.br; lfpires@simpipe.com; cveloso@simdut.com.br

A. O. Nieckele (✉)
Department of Mechanical Engineering, PUC-Rio (Pontifical Catholic University of Rio de Janeiro), Rio de Janeiro, Brazil
e-mail: nieckele@puc-rio.br

ABCM – Brazilian Society of Mechanical Sciences and Engineering et al. (eds.),
Handbook of Pipeline Engineering, https://doi.org/10.1007/978-3-031-05735-9_5-1

Abstract

Thermo-hydraulic simulation of a pipe flow implies in the numerical determination of the flow field and temperature distribution to evaluate flow rates, pressure drop, and heat loss. The numerical prediction of the flow for a given configuration can be applied during pipeline design, to define the pipe characteristics (pipe diameter, thickness, material, insulation), to determine the required pumping power, or to plan pipeline inspection gauge (PIG) launching sites. The numerical solution of the flow field can also be useful during pipeline operation, to control and plan supply and demand requirements, optimizing the process. A numerical real-time solution can also be applied as didactic tool for pipeline operator training purposes, after performing model validation and communication with the supervisory software. In the following sections, after a brief introduction, the necessary mathematical modeling and numerical strategies are presented. In the sequence, a few typical examples are described.

Keywords

Liquid pipeline · Gas pipeline · Mathematical model · Numerical model · Components model · Thermo-hydraulic simulation

Introduction

There are several situations where the flow prediction can be useful. From the point of view of the problem to be simulated, some situations that can be sought are:

- Design of a new pipeline, based on supply and demand conditions
- Verify certain operating condition of an existing pipeline
- Expansion project for an existing pipeline due to changes in supply or demand
- Operation optimization
- Operator training
- Leak detection

More specifically, the simulation also allows the analysis of the following situations:

- Pipeline start and stop procedures
- Operating standards for compressors or pumps
- Determination of survival time of gas distribution systems
- Operators training and evaluation

- System response to failure conditions and determination of corrective strategies
- Prediction of environmental impact from potential leakage and spill volumes
- Batch tracking
- Design of surge control systems
- Pig displacement operations for flow assurance or integrity evaluation
- Effects of pipeline rupture

To properly use a simulator, it is necessary to understand the physical-mathematical model and the numerical model on which the simulator is based. However, what is expected of a professional is to assess the relevant details of the problems that must be addressed and, after running the program, to know how to evaluate the obtained result, interpreting it and verifying what is consistent or not in these results.

There are a large number of different simulation packages on the market, and it can be a challenge to select the right computer program, decide when and exactly what to use it for. So, the primordial question is: for which application the pipeline flow simulator is needed? Therefore, identification of the proper conditions to be analyzed must be done before choosing the software.

A simulator can be classified according to the time dependency (transient or steady state) and/or by the number of phases present in the flow (single-phase versus multi-phase simulators). Further, the simulator can have real-time solution capabilities, which is important for training pipeline operators.

Some simulation packages are built to solve only steady-state flow. These simulations are simpler and faster. They can be useful to analyze the pressure and temperature distribution along the pipeline, or, for example, for pipeline network, as illustrated in Fig. 1.

To analyze a pipeline flow when there is any change in operations condition, that is, to analyze the system evolution from one state to another, a transient simulator must be employed. Nevertheless, they are often more complex and require more computing time.

The first generation of computer programs for simulating flow in pipes was developed to deal with single phase flow of water or steam flow in pipelines. With the growth of the industry needs and natural evolution of technology and physical modeling of the phenomenon, multiphase simulators became viable. The production flows in oil well columns are typical applications for these computer programs, as they often involve multiphase flow of oil, gas, and water.

Due to its intrinsic characteristics, single phase flow simulators usually are more robust, faster, and easier to use. Liquid flows along pipelines are predominantly single-phase, however, it may occur that at some point in the pipeline, the pressure is reduced below the bubble point, forming steam pockets, interfering with the flow.

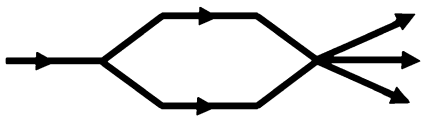

Fig. 1 Pipeline network

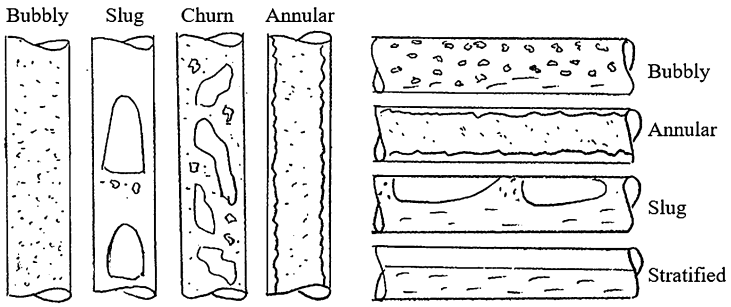

Fig. 2 Flow configurations for vertical and horizontal pipes

Thus, some single-phase simulators may have built-in models to handle this event, when it is observed in small sections of the pipeline. The same is true for a gas flow, as during a depressurization operation, condensate can be formed.

Multiphase flows are transient in nature, presenting different flow patterns, that is, phases distribution, like stratified, slug, annular, bubbly, churn, etc., as shown in Fig. 2 (Brennen 2005). The additional flow complexity related to the flow pattern leads to several different approximations to analyze this type of flow, and specific software are required.

When to use a specific simulator, or which computer program should be chosen in the different stages of a project? The initial stage of a pipeline design can allow relatively simple calculations, and in these cases, steady state simulators can be used. In the later stages of the project, analyses involving transients are needed and more sophisticated simulators are desired. After pipeline construction, in the operational stage, other demands are required such as operator training and leak detection. Thus, using the same software during as many project stages as possible reduces the team's need to become familiar with several different interfaces. Thus, a careful analysis of costs and benefits must be carried out for the selection of the simulation program. Should it be a commercial software, or should it be developed?

To determine a flow field, for a given set of boundary conditions and initial state, conservation equations must be solved. Since these equations are nonlinear and coupled, numerical solution is necessary. In the next sections, both subjects are addressed.

Mathematical Modeling for Pipeline

The governing equations to determine velocity (u), pressure (P), and temperature (T) are the conservation equations of mass, momentum, and energy (Bird et al. 2015). For the particular case of pipelines, the flow can be modeled as one-dimensional, due to the small diameter-to-length ratio of the pipelines. As previously mentioned, the flow can be single phase or multi-phase. The conservation equations can be written for a finite control volume, as indicated in red in Fig. 3, where the pipe diameter is D.

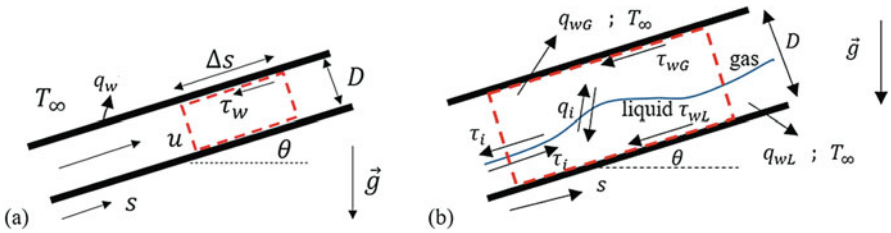

Fig. 3 Pipeline domain. (**a**) Single phase. (**b**) Two phase

Figure 3a illustrates a single-phase domain and Figure 3b, a particular case of two-phase flow domain. The pipe can be inclined of an angle θ in relation to the horizontal direction, $\vec{g}$ is the gravity acceleration vector, s is the flow direction, T_∞ is the ambient temperature, and q_w is the heat flux lost from the fluid to the ambient.

To solve the set of conservation equations, one needs to specify boundary and initial conditions for each conservation equation. Additional information related to the viscous stress τ, heat transfer q, and pipeline dilatation due to pressure must also be informed.

To complete the modeling, fluid properties must be defined. As expected fluid properties exhibit significantly different behavior, depending on whether the fluid is a liquid or a gas, or a multi-phase mixture.

Single-Phase Flow Model

The conservation equations of mass and linear momentum (Newton's second law) for single phase flow (Figure 3a) can be written as

$$\frac{\partial \rho A}{\partial t} + \frac{\partial \rho u A}{\partial s} = 0 \tag{1}$$

$$\frac{\partial \rho u A}{\partial t} + \frac{\partial \rho u^2 A}{\partial s} = -A\frac{\partial P}{\partial s} - \rho g \sin\theta A - \tau_w S_w \tag{2}$$

where ρ is the fluid density, t is time, $A = \pi D^2/4$ is the cross-sectional area and $S_w = \pi D$ is the wall wetted perimeter. For isothermal flow, only these two conservation equations are necessary. However, if there is temperature change, the energy equation must also be solved. The 1D energy equation can be written, based on temperature, as

$$\frac{\partial \rho u A T}{\partial t} + \frac{\partial \rho u A T}{\partial s} = -\frac{q_w \pi D}{c_p} + \frac{\beta T}{c_p} A \frac{DP}{Dt} + \frac{\partial}{\partial s}\left(k A \frac{\partial T}{\partial s}\right) + \frac{\Phi}{c_p} \tag{3}$$

Here, the properties are: c_p – specific heat at constant pressure, k – thermal conductivity, and β – thermal expansion coefficient. $D/D\,t = \partial/\partial\,t + u\,\partial/\partial\,s$ is the

material derivative. The last two terms of the equation correspond to the axial diffusion flux and viscous dissipation ($\Phi = \tau_w\ S_w\ u$). Additional simplifying hypotheses are often introduced in the energy equation, and usually these two terms are neglected. However, the viscous dissipation can play an important hole for high velocity or high viscous flow.

Two-Phase Flow Models

When dealing with two-phase flow, there is an additional challenge, which is the identification of the phase spatial distribution. The phase distribution depends directly on the fluids properties, flow rate of each phase, geometric parameters such as pipe diameter and inclination, etc. As shown in Fig. 2, there is a wide variety of flow patterns that can be formed. The phases are identified by their respective volume fraction:

$$\alpha_\ell = \frac{\forall_\ell}{\forall} = \frac{A_\ell}{A};\ \sum_{\ell=1}^{n} \alpha_\ell = 1 \tag{4}$$

where $\forall = A\ ds$ represents the volume, A the cross-section area, and the subscript ℓ indicates the phase (gas G or liquid L).

There are several different models to predict two-phase flow, therefore, there are also several types of simulators. Some models are designed for a particular type of flow pattern. Here, a quick overview of three models is presented.

Two-Fluid Model

The multi-fluid model (Ishii and Hibiki 2006) is based on a set of conservation equations for each fluid (or phase) present inside the pipe, where ℓ can be different liquids (like oil and water) and/or gas. For the particular case of existing only two phases, it is named Two-Fluid model. Considering Figure 3b, the conservation equations of mass, momentum, and energy (in terms of enthalpy h), can be written for each phase ℓ as:

$$\frac{\partial}{\partial t}(\rho_\ell \alpha_\ell) + \frac{\partial}{\partial s}(\rho_\ell \alpha_\ell\ u_\ell) = \pm \Gamma_\ell\ ; \qquad \sum_{\ell=1}^{n} \Gamma_\ell = 0; \ell = G \text{ and } L \tag{5}$$

$$\frac{\partial(\rho_\ell \alpha_\ell\ u_\ell)}{\partial t} + \frac{\partial\left(\rho_\ell \alpha_\ell\ u_\ell^2\right)}{\partial s} = -\alpha_\ell \frac{\partial\ P_\ell}{\partial s} + (P_{i\ell} - P_\ell)\frac{\partial\ \alpha_\ell}{\partial s} - \rho_\ell \alpha_\ell\ g \sin\theta - \frac{\tau_{w\ell} S_\ell}{A} \pm \frac{\tau_i S_i}{A} \pm \Gamma_\ell u_\ell \tag{6}$$

$$\frac{\partial(\rho_\ell \alpha_\ell h_\ell)}{\partial t} + \frac{\partial(\rho_\ell \alpha_\ell u_\ell h_\ell)}{\partial s} = \alpha_\ell \frac{D_\ell P_\ell}{Dt} + (P_{i\ell} - P_\ell)\frac{D\,\alpha_\ell}{Dt} - \frac{q_{w\ell}\, S_{w\ell}}{A} \pm \frac{q_i\, S_i}{A} + \frac{\tau_{w\ell} S_{w\ell}}{A}\, u_\ell + \frac{\tau_i\, S_i}{A}(u_G - u_L) \pm \Gamma_\ell h_\ell \tag{7}$$

where the subscript i corresponds to interface. Γ_ℓ is the mass flux between the phases, due per example of phase change. Closure expressions are needed here to determine the fluid properties, shear stress τ, and heat flux q. Additional closure equations with respect to the difference between the interface and average pressure $(P_{i\ell} - P_\ell)$ of each phase are also necessary. Further, expressions to estimate the interface curvature κ are needed to determine the difference between the interface pressure phases $(P_{iG} - P_{iL}) = \sigma\,\kappa$, where σ is the surface tension.

Drift Model

The drift flux model employs a mass conservation equation for each phase and a mixture conservation equation for momentum and energy. The mixture equations are obtained by summing the phase equations shown for the two-fluid model, resulting in

$$\frac{\partial}{\partial t}(\rho_\ell \alpha_\ell) + \frac{\partial}{\partial s}(\rho_\ell \alpha_\ell\, u_\ell) = \pm\Gamma_\ell;\ \sum_{\ell=1}^{n} \Gamma_\ell = 0; \ell = G \text{ and } L \tag{8}$$

$$\frac{\partial(\rho_m\, u_m A)}{\partial t} + \frac{\partial\left(\rho_m\, u_m^2 A\right)}{\partial s} = -A\frac{\partial\, P}{\partial s} - \rho_m\, g\, A \sin\theta - \tau_w S_w - \frac{\partial(\,J\, u_r\, A)}{\partial s} \tag{9}$$

$$\frac{\partial(\rho_m h_m A)}{\partial t} + \frac{\partial(\rho_m u_m h_m A)}{\partial s} = A\,\frac{DP}{Dt} - q_w\, S_w + \tau_w\, S_w\, u_m + \left(\alpha_G\,\alpha_L\,\frac{\rho_L - \rho_G}{\rho_m}\,u_r\right) A\,\frac{\partial P}{\partial s} - \frac{\partial}{\partial \mathrm{s}}\,[A\,J\,(h_G - h_L\,)] \tag{10}$$

where

$$J = \alpha_G\,\alpha_L\,\frac{\rho_G\,\rho_L}{\rho_m}\,u_r\ ;\ u_r = u_G - u_L = \frac{V_{Gj}}{\alpha_L} \tag{11}$$

The phase velocities can be obtained from the mixture velocity with

$$u_G = u_m + \frac{\rho_L}{\rho_m}\,V_{Gj}\ ;\ u_L = u_m - \frac{\alpha_G}{\alpha_L}\,\frac{\rho_G}{\rho_m}\,V_{Gj} \tag{12}$$

There are several empirical correlations to determine V_{Gj}, which depend on the flow pattern (Beggs and Brill 1984)

$$V_{Gj} = V_{\text{drift}} + (C_o - 1)\,j\ ;\ j = u_{sG} + u_{sL}; u_{s\ell} = \alpha_\ell\, u_\ell \tag{13}$$

where $u_{s\ell}$ is the phase ℓ superficial velocity. Empirical correlations for the distribution parameter C_o and the drift velocity V_{drift} usually depend on the volume fraction α_ℓ.

Homogeneous Model

A simplified approach for the two-phase flow model is the homogenous model, where the relative velocity of the drift flux model is set to zero, and the mixture conservation of mass is obtained by summing the phase mass conservation equations, resulting in

$$\frac{\partial}{\partial t}(\rho_m A) + \frac{\partial}{\partial s}(\rho_m\, u_m\, A) = 0 \tag{14}$$

$$\frac{\partial(\rho_m\, u_m A)}{\partial t} + \frac{\partial\left(\rho_m\, u_m^2 A\right)}{\partial s} = -A\frac{\partial\, P}{\partial s} - \rho_m\, g\, A \sin\theta - \tau_w S_w \tag{15}$$

$$\frac{\partial(\rho_m h_m A)}{\partial t} + \frac{\partial(\rho_m u_m h_m A)}{\partial s} = A\,\frac{DP}{Dt} - q_w\, S_w + \tau_w\, S_w\, u_m \tag{16}$$

Closure Models

To complete the set of conservation equations, viscous shear stress, and heat transfer to the ambient must be defined. Pipe dilatation is also often considered, due to high pressures. Examples of these closure parameters are shown in the next sub-sections.

For two-phase flow, depending on the model, additional quantities related to the interface, such as shear stress, heat flux, and relative velocity must also be defined. These quantities also depend on the flow pattern.

Friction Factor

The wall friction stress, τ_w, is determined based on Darcy friction factor f, by assuming a local fully developed flow (Pritchard and Mitchell 2015)

$$\tau_w = \frac{f}{8}\,\rho\, u\, |u| \tag{17}$$

f is dependent on the Reynolds number

$$\text{Re} \;=\; \rho|\, u\,|\, D/\mu \tag{18}$$

where μ is dynamic viscosity. In Eq. (17), the absolute value of the velocity is employed, to be able to predict positive and negative flow, that is, the shear stress must always be opposite to the flow direction. For laminar regime $\text{Re} \leq 2300$, $f = 64/\text{Re}$. For turbulent regime, the friction factor is also a function of the relative roughness, ε/D, and different correlations can be employed, like Haaland (1983) equation (Pritchard and Mitchell 2015):

$$\frac{1}{\sqrt{f}} = -1.8\ \log\left[\left(\frac{\varepsilon/D}{3.7}\right)^{1.11} + \frac{6.9}{\mathrm{Re}}\right],\ \mathrm{Re} > 2300 \tag{19}$$

As an alternative, the Swamee (1993) equation, which is valid for the whole range of Reynolds number from laminar flow to complete turbulent flow as well as the transition in between them, can be employed:

$$f = \left\{\left(\frac{64}{\mathrm{Re}}\right)^{8} + 9.5\left[\log\left(\frac{\varepsilon/D}{3.7} + \frac{5.74}{\mathrm{Re}^{0.9}}\right) - \left(\frac{2500}{\mathrm{Re}}\right)^{6}\right]^{-16}\right\}^{0.125} \tag{20}$$

Equivalent shear stress expressions can be applied for the homogeneous and drift flux model. For the two-fluid model, the shear stresses at the wall and interface are

$$\tau_{w\ell} = \frac{f_\ell}{8}\,\rho_\ell\,u_\ell\,|u_\ell|; \qquad \tau_i = \frac{f_i}{8}\,\rho_G\,(u_G - u_L)\,|u_G - u_L| \tag{21}$$

f_ℓ and f_i are functions of the phase and interface Reynolds numbers, respectively, depending on the flow regime and flow pattern, and several empirical correlations can be employed.

Heat Transfer to the Environment

To assess the heat loss of the fluid inside the pipe to the environment, two approaches can be considered. In the first one, the concept of equivalent resistance is applied, considering steady state regime to evaluate the heat transfer through the pipe wall (Incropera et al. 2007). In the second approach, the energy stored at the insulating layers is considered, and the transient variation of the temperature is determined (Incropera et al. 2007).

In both approaches, the heat transfer coefficient from the fluid inside the pipe to the wall (h_{in}) and the external heat transfer coefficient from the external pipe wall to the environment (h_{ex}) are needed. There are several correlations to evaluate the heat transfer coefficients, and examples to determine the inner and external heat transfer coefficients are presented in the sequence. Usually, the heat transfer coefficient is defined based on the Nusselt number, $Nu = h\,L_c/k$, where L_c is a characteristic length.

Steady State at the Insulating Layers

In a pipeline the heat transfer from the flowing fluids inside the pipe to the outside environment will possibly cross different layers with different areas. Using the inner pipe diameter D to calculate the reference area, the heat flux defined as the heat flow divided by the reference area, $q_w = q/(\pi DL)$, can be obtained as

$$q_w = U_G\,(T - T_\infty) \tag{22}$$

where T_∞ is the ambient temperature and U_G is the overall heat transfer coefficient [$W/(m^2K)$ or $Btu/(h\ ft^2\ R)$], based on the inner pipe diameter D. Usually, it presents three contributions: (i) internal convective thermal resistance, $\mathrm{Res}_{\mathrm{in}}$, (ii) pipe conduction thermal resistance, due to its several layers, Res_k, (iii) external thermal resistance $\mathrm{Res}_{\mathrm{ex}}$

$$U_G = \frac{1}{\pi\, D\, L\, (\mathrm{Re\,s}_{in} + \mathrm{Re\,s}_k + \mathrm{Re\,s}_{\mathrm{ex}})} \tag{23}$$

The internal thermal resistances is

$$\mathrm{Re\,s}_{\mathrm{in}} = \frac{1}{h_{\mathrm{in}}\, \pi\, D\, L} \tag{24}$$

where h_{in} is the internal convection heat transfer coefficient, depending on the flow condition inside the pipe.

Since the pipeline can have several layers, the conduction thermal resistance depends on the thermal conductivity of each layer k_n, as well as each layer thickness e_n as

$$\mathrm{Re\,s}_k = \sum\nolimits_{n=1}^{N} \frac{\ln[(D_n + 2e_n)/D_n]}{2\, \pi\, L\, k_n} \tag{25}$$

In Eq. (25), the pipe wall is considered as $n = 1$ and $n > 1$ for all additional layers. N is the total number of layers. Note the first diameter D_1 corresponds to the pipe inner diameter D (radius r_{in}).

The external thermal resistance, also referred as conduction shape factor, is

$$\mathrm{Re\,s}_{\mathrm{ex}} = \frac{1}{h_{\mathrm{ex}}\, \pi\, D_{\mathrm{ex}}\, L}; D_{\mathrm{ex}} = D_N + 2e_N = 2\, r_{\mathrm{ex}} \tag{26}$$

with h_{ex} as the external heat transfer coefficient, which must be specified based on the external environment, depending on if the pipeline is immersed in a fluid (convection) or buried (conduction).

Combining the previous expressions, the overall heat transfer coefficient based on the inner pipe area can be written as

$$U_G = \frac{1}{\left(\frac{1}{h_{in}} + D \sum\nolimits_{n=1}^{N} \frac{\ln[(D_n+2e_n)/D_n]}{2\ k_n} + \frac{D}{h_{ex}\ D_{ex}}\right)} \tag{27}$$

Alternative forms of the overall heat transfer coefficient can be found in the literature as the Global Heat Transfer Coefficient [$W/(m\ K)$ or $Btu/(h\ ft\ R)$]

$$U_o = U_G\, r_{\text{in}} = \frac{1}{\left(\frac{1}{h_{\text{in}}\, r_{\text{in}}} + \sum_{n=1}^{N} \frac{\ln[(D_n+2e_n)/D_n]}{k_n} + \frac{1}{h_{\text{ex}}\, r_{\text{ex}}}\right)} \tag{28}$$

and thermal exchange coefficient (TEC $= U_o\, 2\,\pi$), usually employed in the petroleum industry.

Transient Regime at Insulating Layers

The transient regime at insulating layers approach is usually recommended when the thermal capacity of the system is high, resulting in a long-time interval to attain steady state condition.

To determine the heat transfer through the layers, considering the energy storage in them, the energy conservation equation, particularized for conduction, is solved, along the radial direction, for each axial coordinate of the duct:

$$\rho_i\, cp_i \frac{\partial\, T_i}{\partial\, t} = \frac{1}{r}\, \frac{\partial}{\partial\, r}\left(r\, k_i \frac{\partial T_i}{\partial r}\right); 1 \le i \le N \tag{29}$$

This equation is solved, employing continuity of heat flux between the layers, with the following inner and outer layer boundary conditions

$$r = r_{\text{in}} = \frac{D}{2}; -k_1 \frac{\partial T_1}{\partial\, r}\Bigg)_{\text{in}} = q_w \tag{30}$$

$$r = \frac{D_{\text{ex}}}{2}; -k_N \frac{\partial T_N}{\partial\, r}\Bigg)_{\text{ex}} = h_{\text{ex}}\, (T_{\text{ex}} - T_\infty) \tag{31}$$

where T_{ex} is the external temperature of layer N. In this case, the heat flux lost by the fluid is defined with respect to the inner pipe wall temperature T_w, based on the internal convection heat transfer coefficient h_{in}

$$q_w = h_{in}\, (T - T_w) \tag{32}$$

Internal Heat Transfer Coefficient

The inner convective heat transfer coefficient, $h_{in} = Nu_{\text{in}}\, k/D$, depends directly on the flow in the inner pipe. In most situation, forced convection is the dominant heat transfer mechanism, but for very slow flows, natural convection can play a hole. Further, the flow can be laminar or turbulent, depending on the Reynolds number.

For forced convection laminar regime (Re $\le$ 2300), $Nu_{\text{in}} = 3.66$ for constant wall temperature and $Nu_{\text{in}} = 4.36$ for constant heat flux. For turbulent regime, Nu_{in} can be obtained as a function of the Reynolds number, Re, and Prandtl number, Pr $= \mu\, c_p/k$. There are several correlations that can be employed, depending on the range of Re and Pr (Incropera et al. 2007), like

- Dittus-Boelter ($\mathrm{Re} > 10^4$; $0.6 \leq \mathrm{Pr} \leq 160$; $L/D \geq 10$; $n = 0.4$ fluid heated, $n = 0.3$ cooled)

$$Nu_{\mathrm{in}} = 0.0023\ \mathrm{Re}^{4/5}\ Pr^{n} \tag{33}$$

- Gnielinski ($3000 \leq \mathrm{Re} \leq 5 \times 10^6$, $0.5 \leq \mathrm{Pr} \leq 2000$):

$$Nu_{\mathrm{in}} = \frac{(f/8)(\mathrm{Re} - 1000)\ \mathrm{Pr}}{1 + 12.7\ (f/8)^{1/2}\left(\mathrm{Pr}^{2/3} - 1\right)} \tag{34}$$

Natural convection is important when $\mathrm{Gr}/\mathrm{Re}^2 > 1$, where $Gr = \rho g\, \beta\, (T - T_w) D^3/\mu$ is the Grashof number and the Nusselt number can be determined with Oliver correlation (Holman 2010)

$$Nu_{\mathrm{in}} = 0.354 \left(\frac{\mu_w}{\mu}\right)^{0.14} (\mathrm{Gr}\ \mathrm{Pr})^{1/4} \tag{35}$$

In an analogous form as described for the shear stress, the internal convective heat transfer coefficient h_{in} can be empirically determined for the mixture, phase, and interface to obtain the heat flux lost by the fluid [$q_w = h_{in}\,(T - T_w)$; $q_{w\ell} = h_{in,\,\ell}\,(T - T_{w\ell})$; $q_i = h_i\,(T_G - T_L)$].

External Heat Transfer Coefficient for Aerial or Submerged Pipes

When the pipeline is aerial or submerged, h_{ex} can be calculated from the Hilpert correlation (Incropera et al. 2007)

$$h_{\mathrm{ex}} = \frac{k_\infty}{D_{\mathrm{ex}}}\left[C\ \mathrm{Re}_\infty^{m}\mathrm{Pr}_\infty^{1/3}\right];\ \mathrm{Re}_\infty = \frac{\rho_\infty\, V_\infty\, D_{\mathrm{ex}}}{\mu_\infty};\ \ \mathrm{Pr}_\infty = \frac{\mu_\infty\, c_{p,\infty}}{k_\infty} \tag{36}$$

where ρ_∞, μ_∞, k_∞, and $c_{p,\,\infty}$ are the specific mass, absolute viscosity, thermal conductivity, and specific heat at constant pressure of the fluid in the external medium. V_∞ is the velocity of the external current. Table 1 presents the values of m and C according to Reynolds of the external environment Re_∞.

External Heat Transfer Coefficient for Buried Pipes

For long buried pipes ($L \gg D_{ex}$) in horizontal position (Fig. 4a), the external heat transfer coefficient can be determined considering a semi-infinite medium as (Incropera et al. 2007):

Table 1 Hilpert correlation parameters

Re_∞	C	m
4×10 to 4×10^3	0.683	0.466
4×10^3 to 4×10^4	0.193	0.618
4×10^4 to 4×10^5	0.027	0.805

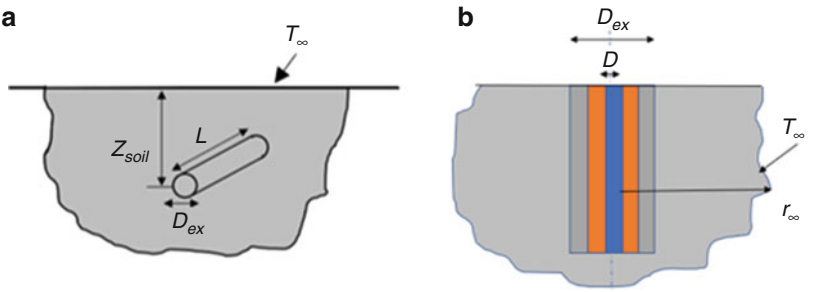

Fig. 4 Horizontal pipe and vertical well buried pipe in semi-infinite medium. (**a**) Horizontal. (**b**) Vertical buried well

$$\text{horizontal}: h_{\text{ex}} = \frac{1}{\frac{D_{\text{ex}}}{2\,k_{\text{soil}}}\cosh^{-1}\left(\frac{2\,z_{\text{soil}}}{D_{\text{ex}}}\right)} \text{ or } h_{\text{ex}} = \frac{1}{\frac{D_{\text{ex}}}{2\,k_{\text{soil}}}\ln\left(\frac{4\,z_{\text{soil}}}{D_{\text{ex}}}\right)} \text{ if } \frac{z_{\text{soil}}}{D_{\text{ex}}} > 1.5 \quad (37)$$

where k_{soil} is the thermal conductivity of the soil and z_{soil} is the depth at which the pipe is buried (Fig. 4) and L is the pipe lenght.

External Heat Transfer Coefficient for Pipes Buried Perpendicular to the Ground – Wells

To evaluate the thermal resistance of external surface of a well in relation to the formation (Fig. 4b), one can also consider a semi-infinite medium. In the formation a temperature gradient that varies with time can be observed, due to the heat transfer from the well, but at a certain time $\boldsymbol{t}$, and a radial position $\boldsymbol{r}_\infty$ far enough from the well the formation temperature is not affected by the well. Based on this assumption Hasan and Kabir (2018) recommended the following procedure to calculate the external heat transfer coefficient, employing a dimensionless time defined as

$$t_D = \frac{4\,\alpha_{\text{form}}\,t}{D_{\text{ex}}^2}; \alpha_{\text{form}} = \left(\frac{k}{\rho\,cp}\right)_{\text{form}} \quad (38)$$

where k, ρ, and cp are the thermal conductivity, density, and specific heat of the formation. The external heat transfer coefficient can be obtained from

$$h_{\text{ex}} = \frac{2\,k_{\text{form}}}{D_{\text{ex}}\,[0.4063 + 0.5\ln(t_D)]\left(1 + \frac{0.6}{t_D}\right)} \text{ if } t_D > 1.5 \quad (39)$$

$$h_{\text{ex}} = \frac{2\,k_{\text{form}}}{D_{\text{ex}}\,1.1281\,\sqrt{t_D}(1 - 0.3\sqrt{t_D})} \text{ if } t_D \leq 1.5 \quad (40)$$

Pipeline Wall Expansion

There are some situations that involve high pressure, resulting in pipeline deformation, and it must be accounted for. Thus, the pipe diameter can be determined from (Wylie and Streeter 1978)

$$D = \frac{D_{\text{ref}}}{1 - C_D\,(P - P_{\text{atm}})}; C_D = \frac{1 - \nu^2}{2\,e\,E}\,D_{\text{ref}} \tag{41}$$

where D and D_{ref} are the inner pipeline diameter and the reference inner diameter determined at atmospheric pressure P_{atm}. C_D is the pipe deformation coefficient due to pressure. To determine C_D, e is the pipe wall thickness, E is the Young's modulus of elasticity of the pipe material, and ν the Poisson's coefficient.

Fluid Properties

The density can be determined from an equation of state, as a function of pressure and temperature, thus, its variation can be obtained from

$$d\,\rho = \frac{1}{a^2}\,dP - \rho\,\beta\,d\,T; a = \sqrt{\left(\frac{\partial\,P}{\partial\,\rho}\right)_T}; \beta = -\frac{1}{\rho}\left(\frac{\partial\,\rho}{\partial\,T}\right)_P \tag{42}$$

where a is the isothermal speed of sound, and β the thermal expansion coefficient.

Usually, liquids can be considered as incompressible ($\rho \approx$ constant) since β is negligible and a is very large (e.g., water: $a \approx 3000$ m/s). However, if a closing valve operation is being examined, or the pipeline is very long, the variation of density with pressure must be considered. To account to the liquid compressibility, it is usual to employ the bulk modulus, $K = \rho\,(dP/d\,\rho)_T = \rho\,a^2$.

As a first approximation, the ideal gas law can be applied to determine the gas density. It can be corrected for a real gas with a compressibility factor Z, thus the density can be obtained with

$$\rho = \frac{P\,W}{Z\,\Re\,T}; Z = Z(P,T) \tag{43}$$

where $\Re = 8314.5$ J/(kmol K) is the universal gas constant and W is the gas molar weight (kmol/kg). The function $Z(P, T)$ can be determined based on empirical data, or based on different models such as Peng–Robinson, Redlich–Kwong, and Soave–Redlich–Kwong (Poling et al. 2001). For ideal gas, Z=1, $a = \sqrt{\Re\,T/W}$, and $\beta = 1/T$.

For two-phase flow situations, in the presence of phase change, a FLASH procedure (Michelsen and Mollerup 2007) must be employed to determine the mass flux between phases, Γ_k.

Appropriated viscosity, thermal conductivity, and specific heat at constant pressure must be specified for the fluid flowing inside the pipeline. These variables can be defined as constant based on a reference temperature and pressure, or correlations

can be employed. Some simulators offer a database with properties of several different liquids and gases.

Boundary and Initial Conditions

To solve the set of conservation equation, one needs to specify boundary conditions for each conservation equation. Since these equations are first order in the axial direction, only one boundary condition is needed for each one. As mentioned, the energy equation is only solved for non-isothermal flows, and usually the inlet temperature is known, and diffusion flux is neglected at outlet ($\partial\ T/\partial s = 0$). The heat lost to the ambient is treated as described in section "Heat Transfer to the Environment."

Different combinations of boundary conditions can be specified. For example, velocity (or flow rate) and pressure at inlet or both at outlet, or one at the inlet and the other at the outlet, and finally, since velocity and pressure are coupled, pressure can be specified in both ends. In the presence of valves, a relation between mass flow rate $\dot{m}$ and pressure P is required as

$$\dot{m} = \rho\ (C_V\ A_v)\sqrt{2\ \Delta P/\rho} \tag{44}$$

where C_V is the valve discharge coefficient, A_v is the valve cross-section area, $\Delta P = |\ P - P_v|$, and P_v is the reservoir pressure at upstream or downstream of the valve, depending on if the valve is at the inlet or outlet of the pipeline.

When a pump or a compressor is installed at the pipe inlet, its pump curve (or compressor curve) that relates the head (available pressure) with flow rate must be employed. For compressors, temperature is also important.

For transient studies, the initial condition is fundamental, with a direct influence in the solution. If the initial condition corresponds to rest, then velocity is null, and a hydrostatic pressure must be specified. It can also be considered the fluid in thermal equilibrium with the environment. In some applications, the initial condition can be a steady state situation, if per example, the user wants to investigate a pigging operation or the closing of a valve. In these situations, it is necessary to first obtain the steady-state solution before starting the transient analysis.

Numerical Modeling for Pipeline Flow

Since the conservation equations are nonlinear and coupled, an exact analytical solution (valid in all points of space and time) is not possible. Thus, one can search for an approximate solution at discrete points of the domain, and discrete time instants. To this end, each differential equation can be transformed in a set of algebraic equations, valid for each discrete point. There are several methods to transform a differential equation in a set of algebraic equations, like Finite Difference, Finite Volume, Finite Element, Method of Characteristics, etc., and there are

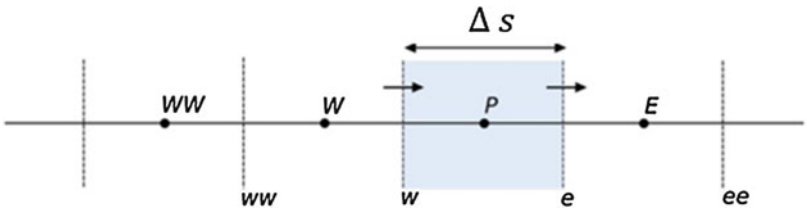

Fig. 5 Notation for nodes and faces on a staggered mesh

also several methods to solve the discretization equations (Versteeg and Malalasekera 2007). A brief idea of the procedure is presented next.

Discretization

The first step to obtain a numerical solution consists in defining discrete points along the domain of interest. As the number of nodal points increases, the solution of the discretization equations is expected to approach the exact solution of the differential equation. Figure 5 illustrates a staggered mesh distribution, where the capital letters indicate the nodal points (P and its neighbors east E and west W sides) and lower case letters indicate the control volume faces, where velocity is stored. The distance between the points, Δs (Fig. 5), can be uniform or non-uniform. The points should be close together when large gradients are expected, and they can be further apart otherwise.

All numerical methods are based on the same concept, that is, to integrate the differential equation in an approximate way, adopting different profiles between the nodes, resulting in a set of discretized algebraic equations, each one associated with each nodal point of the domain. Analyzing the governing equations of section "Mathematical Modeling for Pipeline," one can observe that there are two types of derivative: spatial driven by the velocity field and temporal. To illustrate a discretization procedure, let us consider first the convective term of a variable ϕ, where the mass flow rate is $F = \rho\ u\ A$, and ϕ can be velocity, temperature, etc. Integrating the convective term across the control volume P, from face w to face e, we have

$$\int_w^e \frac{\partial \rho\ u\ A\ \phi}{\partial s}\ ds = F_e\ \phi_e - F_w\ \phi_w \tag{45}$$

To approximate the convective term, an upwind approximation scheme is recommended. It means that information from upstream must have a larger weight than values downstream. The first order upwind scheme is very stable, and very popular:

$$F_e\,\phi_e = [\![F_e, 0]\!]\phi_{\mathrm{P}} - [\![-F_e, 0]\!]\phi_{\mathrm{E}} \tag{46}$$

Here, $[\![a, b]\!]$ means maximum between a and b.

A scheme with second order of approximation is more precise, but also more unstable. An example is the TVD scheme

$$F_e\,\phi_e = [\![F_e, 0]\!]\,\phi_{\mathrm{P}} - [\![-F_e, 0]\!]\phi_{\mathrm{E}} + \frac{1}{2}|Fe|\,\psi(\mathrm{r_e})(\phi_{\mathrm{E}} - \phi_{\mathrm{P}}) \tag{47}$$

where $\psi(r_e)$ is a limiter function, and several expressions are available in the literature, like Van Leer where $\psi(r) = (r+|\,r|\,)/(1\,+\,r)$. The parameter r_e depends on the flow direction as

$$r_e = [\![\mathrm{sign}(u_e), 0]\!]\frac{(\phi_{\mathrm{P}} - \phi_{\mathrm{W}})}{(\phi_{\mathrm{E}} - \phi_{\mathrm{P}})} + [\![-\mathrm{sign}(u_e), 0]\!]\frac{(\phi_{EE} - \phi_{\mathrm{E}})}{(\phi_{\mathrm{E}} - \phi_{\mathrm{P}})} \tag{48}$$

The integration of the temporal term can be represented by the following expression for a large number of schemes

$$\int_t^{t+\Delta t} \phi dt = \left[\phi_i^n\,\omega + \phi_i^{n-1}(1-\omega)\right]\Delta t \tag{49}$$

where the weighing factor ω is different for each scheme. Three very common approaches are: (i) Euler explicit ($\omega = 0$), (ii) Euler implicit ($\omega = 1$), and (iii) Crank–Nicolson ($\omega = 0.5$). The first two are first order of approximation, while the third one is second order. However, scheme 2, Euler implicit is always stable, independent of the size of the time step, while care and restrict time step must be employed with Euler explicit scheme. Crank–Nicolson scheme is more precise, but instabilities can appear during the solution evolution, and restriction on the size of the time step must be defined.

The resulting discretized equation, relating the variable at the nodal point P with its neighboring points nb, can be written in the following form

$$a_P\,\phi_P = \sum_{nb} a_{nb}\phi_{nb} + b \tag{50}$$

The definition of the discretization scheme impacts in the problem precision. Further, the definition of the mesh spacing Δs and time step Δt is very important. The size of the mesh spacing depends on the problem (conservation equations, boundary, and initial conditions) and on the discretization schemes. A grid test must always be performed to guarantee that the solution is mesh independent. The time step must be defined based on the mesh spacing. It is recommended to employ a Courant number $Co \leq 1$, defined as

$$Co = \frac{u_{\max} \Delta t}{\Delta \, s_{\min}} \tag{51}$$

where $u_{\max}$ is the maximum velocity and $\Delta \, s_{\min}$ the smallest mesh spacing.

Solution Procedure

The conservation equations presented are nonlinear and coupled. To solve the coupling, different strategies can be applied. One possibility is to rewrite the conservation equation introducing directly the dependency of the specific mass with pressure and temperature in the continuity equation (Eq. 1), resulting in

$$\frac{DP}{Dt} + \rho \, v_a^2 \left[\frac{\partial u}{\partial s} - \beta \frac{DT}{Dt} \right] = 0 \tag{52}$$

Here v_a is the acoustic wave speed, given by

$$v_a = \sqrt{\frac{a^2}{\xi}} \; ; \; \xi = 1 + \rho a^2 \frac{(1 - \nu^2) D}{2 \, E} \tag{53}$$

One auxiliary vector can be defined as $\Phi = [P, \, u, \, T]^T$ and the set of discretized conservation equation can be solved directly.

Another possibility is to employ an algorithm based on the SIMPLE family (Patankar 1980) like SIMPLEC, PISO, etc. (Versteeg and Malalasekera 2007). The discretized conservation equation of mass and momentum are combined to obtain one equation to correct the pressure, and this correction is also applied to correct the velocity. In this case, the system of conservation equation is solved sequentially.

To solve the system of discretized equations, there also several possible procedures. Since the conservation equations are 1D, usually a direct procedure is applied. The conservation equation can be solved sequentially with Thomas algorithm (Versteeg and Malalasekera 2007), or tri-diagonal matrix algorithm (TDMA). To solve all conservation equations coupled, a block TDMA can be employed, or a penta-diagonal algorithm (for isothermal problems) and hepta-diagonal algorithm (for thermal problems). However, since the equations are nonlinear, an iterative process is needed and a convergence criterion must be defined. The convergence criterion can be based on some specific and relevant variable ϕ_P of the problem, or in the residue *Res* of all conservation equations

$$\left| \, \phi_P - \phi_P^* \right| \leq \text{tol or Res} = \left| a_P \phi_P - \left(\sum_{nb} a_{nb} \phi_{nb} + b \right) \right| \leq \text{tol} \tag{54}$$

These quantities can be the maximum in the domain (more conservative) or average in the domain. To define the tolerance, it is recommended to normalize these expressions, and tolerance *tol* should be smaller than 10^{-3}.

Special Care to Build Models

A pipeline system requires many components to operate in a safe manner. However, some of these components are not required in the numerical model to simulate the pipeline hydraulics. To determine which physical components and hardware on a pipeline can be ignored, the decision should be based on whether the equipment changes the pressure, or the fluid flow or the temperature. On the other side, if the equipment generates a pressure loss, restricts the flow, or changes the fluid properties, the element should probably be included in the model. The evaluation of the equipment is based on the impact on the hydraulics of the pipeline system. A typical example are the main block valves. These valves are full bore type, like gate valves and ball valves and usually are manually operated. They present very little pressure drop when opened and may be dropped from the model. However, if the valve operates partially opened the pressure loss may be significant to the hydraulics and it should be modeled.

In pipeline systems, each of its components, such as pipelines, pumps, valves, compressors, performs a different function, interfering in a specific way in the flow. Thus, it is necessary to identify these components because, in general, simulators deal with these elements according to their characteristics, requiring specific information for their modeling.

However, it should always be seen that in an internal flow there is always a source that supplies the fluid, a pipeline that transports it, and a point that receives this fluid. It can be said that the other elements are "accessories" to the process.

Supply Points

The supplier is the element through which the fluid enters the system. Some simulators only work with liquid or gas. For other simulators, which allow working with both fluids, it is necessary to inform whether the problem to be modeled uses a gas or a liquid. Furthermore, the specific characteristics of the fluid must be informed so that the simulator can calculate its properties.

The fluid supply point is typically modeled to work with a boundary pressure or flow condition, and also inlet fluid temperature depending on thermal modelling. Some simulators accept multiple constraints at supply points, to allow changing between different boundary conditions (maximum pressure, minimal flowrate) during the solution evaluation. In this way, the simulator interprets that the first condition must be met until the second is violated. In this case, the program changes the condition, using the limiting value of the second as the boundary condition.

Reception or Delivery Points

In fluid transport systems, the receiving point usually represents the customer who expects to receive a certain amount of fluid, that is, a customer that has hired to receive a particular product. Following this point of view, the most common

boundary condition when simulating a pipeline is maximum flow. However, for operations with liquid, the reception point is usually in tanks and pressure is the boundary condition most often considered.

Pipelines

Pipelines with a length of hundreds of meters or more must be simulated using pipes with the same characteristics. Each transfer line (pipeline segment) must have similar characteristics, that is, same diameter, roughness, coating, thickness, insulation, etc. If there is any change in these characteristics, or any intermediate equipment that needs to be modelled, the pipeline should be divided into multiple segments, each with uniform characteristics along its length. The terrain elevation profile is simulated using straight pipe segments of constant slope. Each end of a pipeline is called a node. Thus, two pipes are connected when the trail end node of one is the same head end node of the other.

Pipe dimensions are normally based on standards and may vary along the pipeline according to the project needs. Care must be taken with the input diameter requested by the simulator, which can be the inner or outer diameter (in this case the thickness will define the inner diameter, needed for the flow solution). For steel pipes based on the ASME B36.10M-2018, the nominal diameter is the same as the outside diameter for pipes larger than 12″. For diameters equal to or smaller than 12″, the outer diameter must be identified in the tables provided, as shown in Table 2.

Valves

Valves can be connected between two ends of pipes or between pipelines and equipment through nodes. Usually, simulators allow modeling of shut-down valves, check valves (to avoid reverse flow), and control valves (flow or pressure). These devices are characterized by their discharge coefficient (Eq. 44) as a function of the valve opening percentage (Val Matic 2018). It is also related to the valve type and the valve size (Fig. 6).

Pumps (Centrifugal)

Pumps are equipment installed close to supply points, usually in tanks or between two pipeline segments, which provide the energy for product displacement. Normally, simulators allow working with two situations: equipment with some characteristics pre-defined by the program or equipment with characteristics fully provided by the user. The second case should be used when the equipment has already been defined through the characteristics required by the project and the consequent selection of options in the market. Centrifugal pumps area characterized by the

Table 2 Example of dimensions for pipes with nominal diameter of 12″ and 14″

Customary Units				Identification Standard (STD) Extra Strong (XS)			SI Units		
Inch nominal size	Outer diam. in	Wall thick. in	Plain end mass lb/ft	API spec	Extra strong (XXS)	Sched. no	Outer diam. mm	Wall thick. mm	Plain end mass kg/m
12	12.75	0.875	110.97	5L	–	-	323.8	22.23	165.37
12	12.75	0.938	118.33	5L	–	-	323.8	23.83	176.33
12	12.75	1,000	125.49	5L	XXS	120	323.8	25.40	186.97
12	12.75	1,062	132.57	5L	–	-	323.8	26.97	197.48
12	12.75	1.125	139.67	5L	–	140	323.8	28.58	208.14
12	12.75	1,250	153.53	5L	–	-	323.8	31.75	228.74
12	12.75	1,312	160.27	5L	–	160	323.8	33.32	238.76
14	14.00	0.188	27.73	5L	–	-	355.6	4.78	41.35
14	14.00	0.203	29.91	5L	–	-	355.6	5.16	44.59
14	14.00	0.210	30.93	5L	–	-	355.6	5.33	46.04
14	14.00	0.219	32.23	5L	–	-	355.6	5.56	47.99
14	14.00	0.250	36.71	5L	–	10	355.6	6.35	54.69
14	14.00	0.281	41.17	5L	–	-	355.6	7.14	61.35
14	14.00	0.312	45.61	5L	–	20	355.6	7.92	67.90

head versus flow, net positive suction head (NPSH), and power (or efficiency) versus flow curves, as shown in Fig. 7.

Compressors

Compressors are also equipment installed close to gas supply points, or between two pipeline segments, to provide the energy for the gas to move. As for pumps, simulators allow working with two situations: equipment with some characteristics pre-defined by the program or equipment with characteristics fully provided by the user (Fig. 8). For centrifugal compressors, polytropic head versus flow rate curves for various revolutions are typically required. Information such as "surge" and "stonewall" boundaries supplement the input data. Regarding the drives, which can be turbines or engines, consumption and efficiency curves can also be provided.

Solution Quality Evaluation – Liquid Phase Sample Model

The quality of results from numerical methods depends on several factors (Lagoni and Barley 2007). For the users of a commercial thermo-hydraulic pipeline simulation program, most of the parameters that can interfere with the result are inaccessible. Generally, one of the main factors that the user can intervene is the spatial discretization. For most simulation techniques, large discretization reduces the

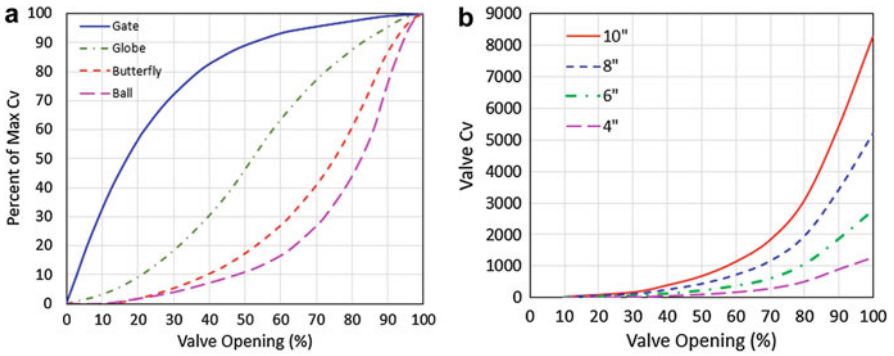

Fig. 6 Valve characteristics: discharge coefficient C_v. (**a**) Maximum C_v. (**b**) C_v for different valve sizes (Butterfly type)

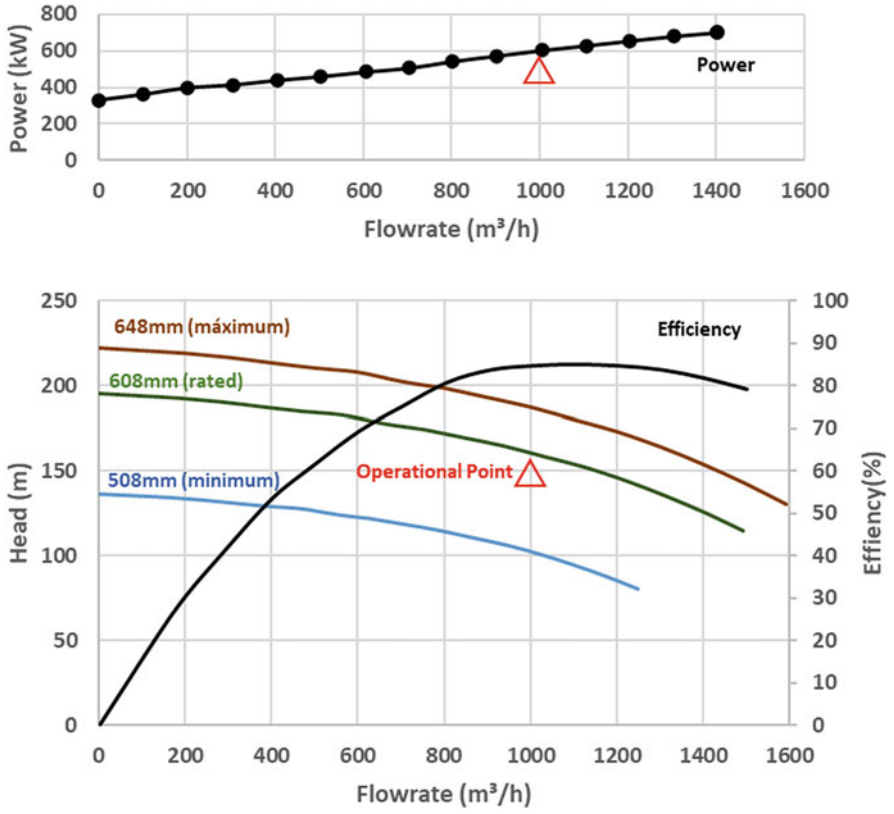

Fig. 7 Characteristic of centrifugal pump curves

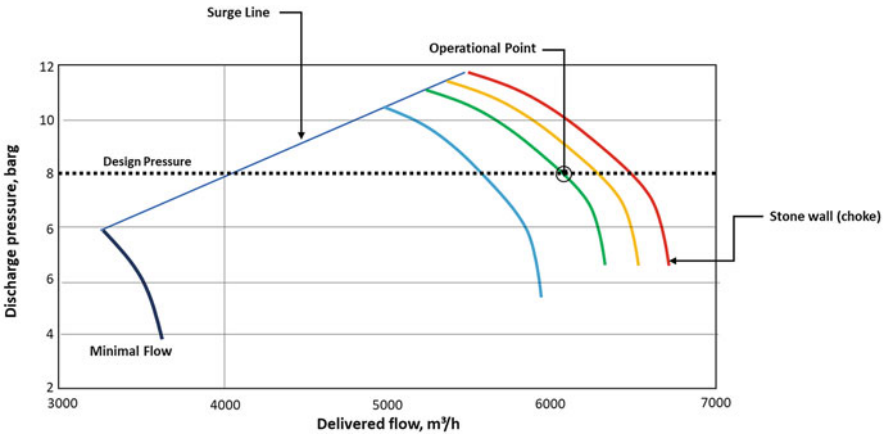

Fig. 8 Centrifugal compressor typical characteristics curve. (Source: Compressed Air and Gas Institute)

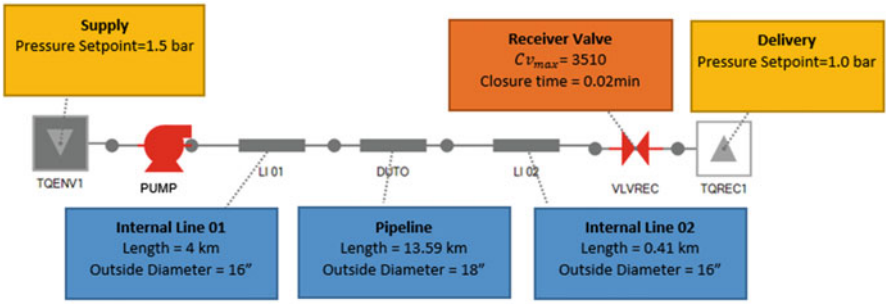

Fig. 9 Solution quality evaluation schematic model

quality of the result. One of the ways to assess how much the spatial mesh is interfering with the result is, after the simulation model is completed, to select the base case of study and vary the mesh size until the result becomes insensitive (within a tolerance) to this variation.

The schematic model shown in Fig. 9 illustrates a pipeline system with a section of 18″ in diameter and 13.59km with two sections of 16″, one at the pump discharge with 4 km and another at the end of the pipeline, with 0.41 km. The elevation profile and maximum allowable operating pressure (MAOP) are shown in Fig. 10a. The transported oil has a density of 811 kg/m^3 and a viscosity of 1.2 cP. The pump has an attached check valve.

The simulated sample scenario represents the instantaneous closure (1 s) of the receiving valve (VLVREC). The results are presented for two numerical formulation techniques: method of characteristics (MOC) and a finite difference model (FDM).

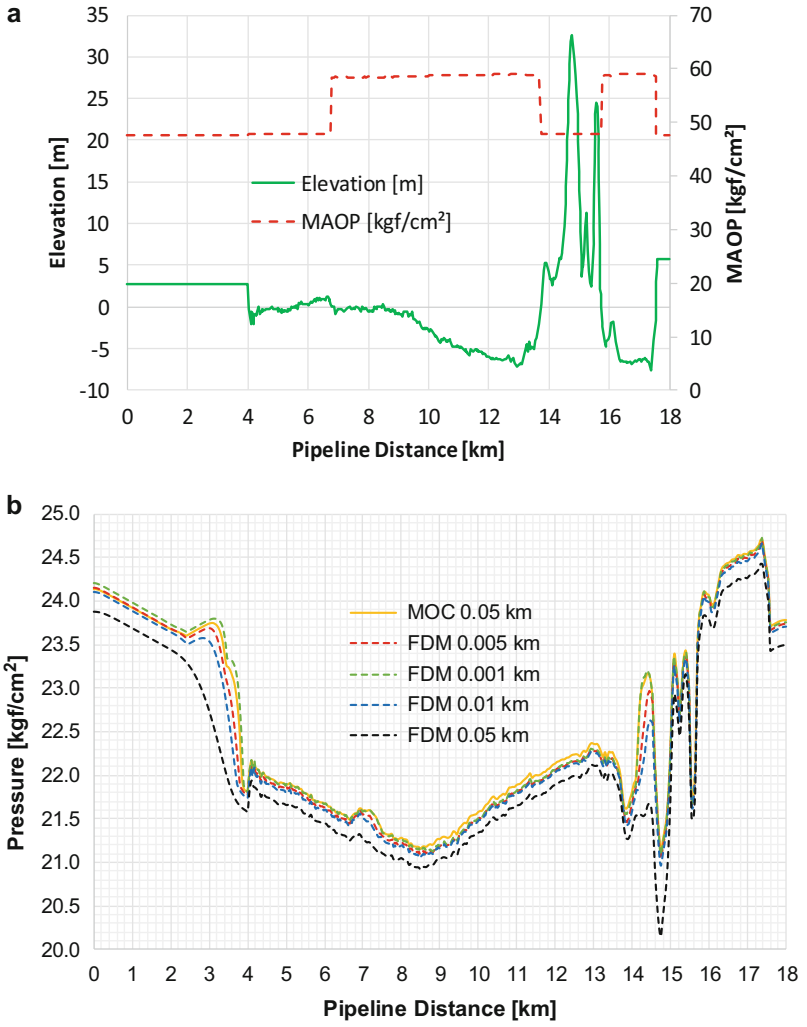

Fig. 10 Maximum pressure along pipeline. (**a**) Pipeline MAOP and elevation profile. (**b**) Maximum pressure profile along the pipe. MOC and FDM

For the MOC, a spatial discretization of 0.05 km was selected and for FDM solutions knot spacing of 0.05 km, 0.01 km, 0.005 km, and 0.001 km were used.

Figure 10b shows the maximum pressure profile along pipe, where mesh convergence of FDM can be observed as the curves collapse and agree with the MOC solution. Figure 11 shows the pressure history at upstream and downstream pipeline nodes. Note that a complex pressure wave pattern is obtained due to the reflections in the diameter variations and the closing of the check valve at the pump discharge. Furthermore, the difference between the results with 0.005 km and 0.001 km mesh is practically imperceptible, indicating that mesh convergence was attained with the 0.005 km mesh.

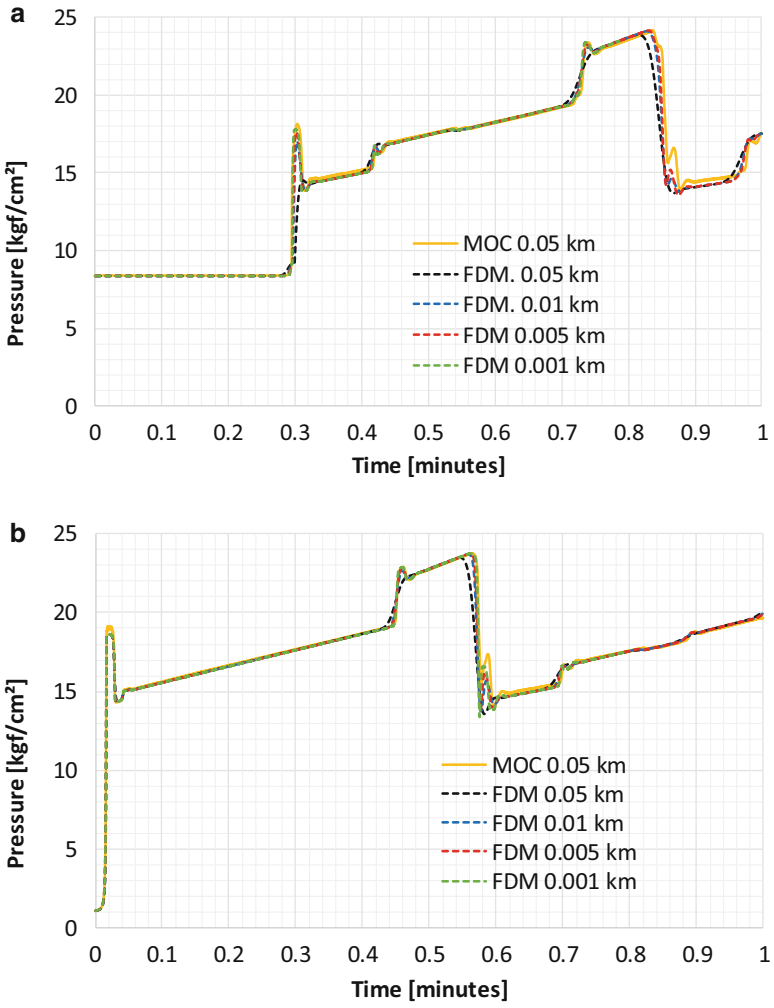

Fig. 11 MOC versus FDM mesh comparison. (**a**) Upstream pressure history. (**b**) Downstream pressure history

Model Tuning for Real Pipeline Conditions

Once the simulation model is prepared and the numerical solution parameters are selected, it is necessary to adjust the model to the real conditions of the pipeline. In addition to the uncertainties associated with the numerical solution, several others parameters, needed to solve the simulation model, are sources that bring uncertainty to the results. As an example, one can mention the equations of state, which provide the specific mass as a function of the pressure and temperature of each fluid, equations that translate the variation of viscosity as a function of temperature,

correlations for calculating the heat transfer coefficient, and for the calculation of the friction factor are the most important.

For existing pipelines, the uncertainties arising from these variables can be reduced through a model adjustment process, where some boundary conditions are introduced into the model from operational data and others are obtained as a result of the calculation and compared with field data. From this comparison, some parameters of the correlations can be adjusted so that the numerical results more faithfully reproduce the real data.

This adjustment can be performed in a simpler way, when field data are obtained in an operational situation where the transport system is operating in a steady state. In the case of a gas transport network, a steady state is very difficult to be identified and in this case the adjustment must be carried out using the operational history in a certain period of time.

As an example, a gas pipeline of about 318 km was used, with diameters of 16″ and 18″ with a supply point and 13 delivery points, as shown in Fig. 12. The model tuning was performed for a period of time of 7 days, where an attempt was made to change the pressure loss by friction along the pipeline, adjusting the pipe roughness. The initial internal roughness of the pipeline was set to 0.0018″.

The analysis of the operational history shows that 5 delivery points work with practically constant flows during the analyzed period and the others present a variable flow as shown in Fig. 13a. These flow profiles were used as input data in the model, as well as the variation of pressure at the supply, as shown in Fig. 13b. Thus, the calculated results provided by the model include the pressure at the delivery points. The pressure at the last delivery point (DP13) was used to calibrate the model, where the roughness of the pipes were varied until obtaining a value that reproduced the real flow behavior. Figure 14 shows the pressure variation obtained from the operational history compared with the results obtained with the initial roughness of the model (0.0018″) and the final adjusted value of 0.0004″.

Typical Applications

Given the wide variety of problems involving pipeline flow simulation (multiphase, single-phase of liquids and gases, non-Newtonian fluids, etc.), this chapter will present some applications of thermo-hydraulics flow simulation, detailing some characteristics and details for the modeling of this phenomenon.

Fast Transient in Pipelines – Liquid Phase Sample Model

A typical application of thermo-hydraulic pipeline simulation is the analysis of fast transients in short liquid pipelines. When building these models, several precautions must be taken because some model details related to equipment characteristics and fluid properties may produce significant differences in the hydraulic simulation results. The transient flow behavior of a pipeline marine terminal during loading

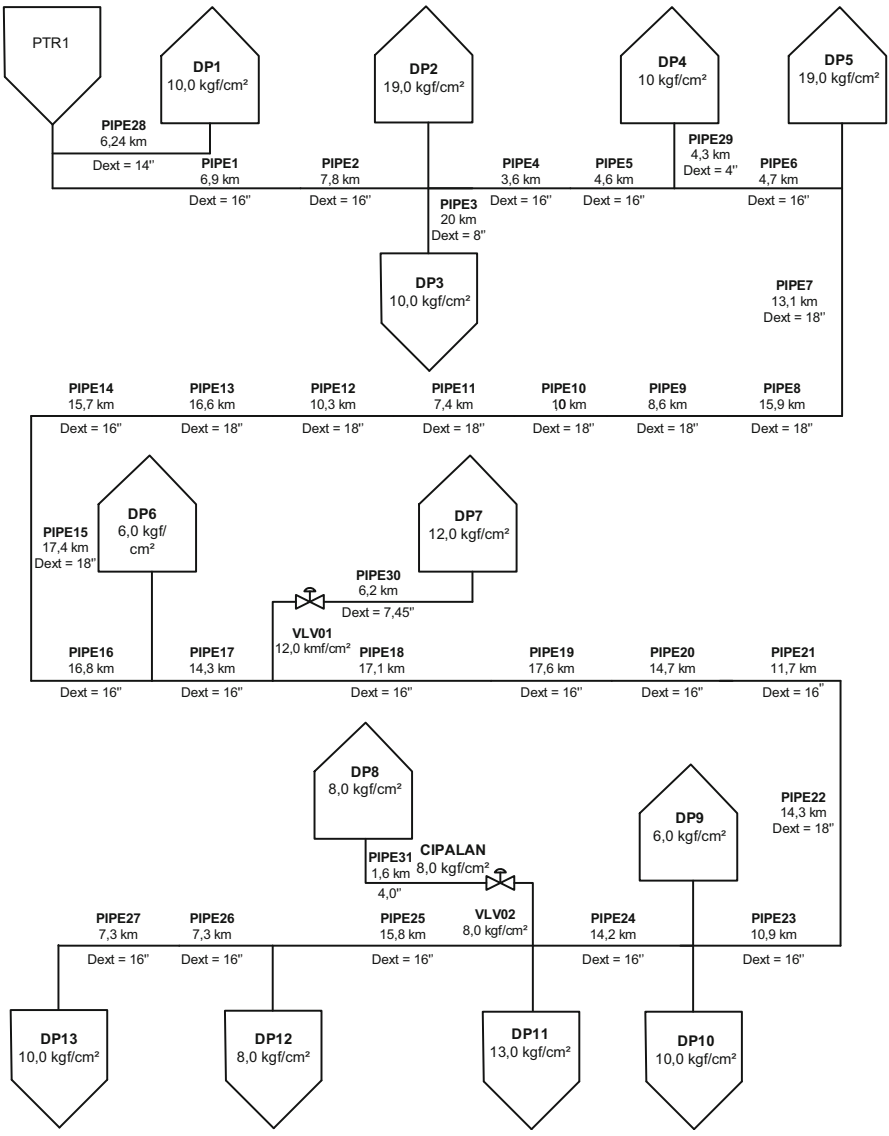

Fig. 12 Schematic of a real gas pipeline network (tuning model sample)

tanker operations was chosen to show this point. The focus of these examples is on transients generated by the rapid closing of a block valve located at the tanker.

Oil and refined product transfer from onshore tanks to ships at marine terminals frequently employs short pipelines, operating at elevated flow rates to minimize dockage time. These pipelines are normally composed by storage tanks, a pumping station, and additional components like control, block, and check valves. Due to the

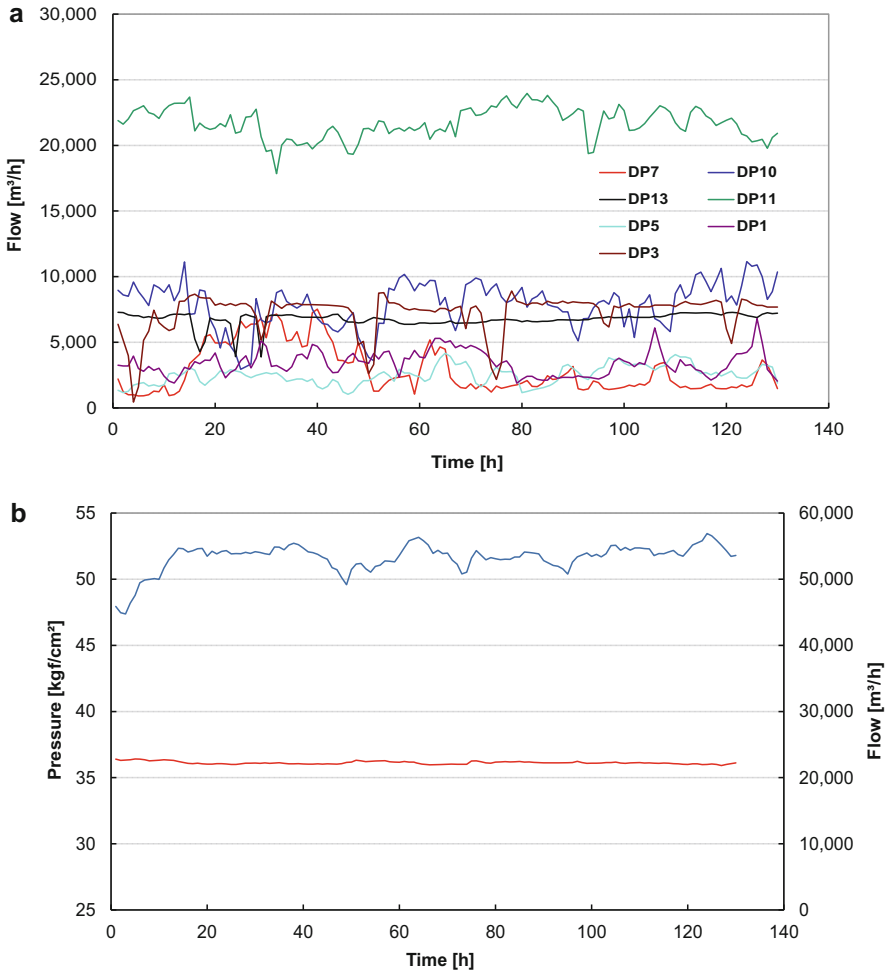

Fig. 13 Flow and pressure time evolution. (**a**) Delivery points' flow trends. (**b**) Flow and pressure trends at supply point

concern with leakages, valves are normally set to operate at very short closing times which, combined with the high flow rates necessary to minimize ship dockage time, may lead to complex fluid flow transients in the system.

The surge pressure ΔP generated by a velocity reduction Δu is usually estimated by a simplified equation, known as Joukowsky's equation ($\Delta P = \rho\ v_a\ \Delta u$), which quantifies the pressure increase in a fluid resulting from a change in velocity Δu, as being proportional to the wave speed, v_a, and the fluid density, ρ. If the flow stops instantly, $\Delta u = Q/A$, where Q is the flow rate prevailing before valve closure. Joukowsky's equation provides an estimate for the pressure surges to be expected in simple transient problems. In actual pipelines, there are several parameters that

affect the intensity of the pressure surge phenomenon, such as fluid velocity, valve discharge coefficient curve, pump performance curves, presence of a check valve, fluid properties, pipeline mechanical properties, etc. The importance to the numerical simulations of some of these parameters will be presented using a sample model.

The pipeline modeled is composed of 3.5 km, of a 16″ outside diameter (OD) rigid line, connected to a 250-m long, 12” OD, flexible hose. Figure 15 presents a schematic representation of the pipeline modeled. The oil flow is driven by a centrifugal pump (BO20), followed by a check valve (BC3), and controlled by a control valve (VCONT). The rigid line (T200) connects the upstream block valve (V1) to the downstream block valve (V02). A 31-m-long subsea rigid line (T210) connects the block valve to the 250-m-long flexible line (T300). A motorized block valve (V9N) connects the flexible line to the tanker. The oil used in the simulations presents a density of 943.7 kg/m^3, an absolute viscosity of 8.3 $\times$ 10^{-3} Pa s, and a

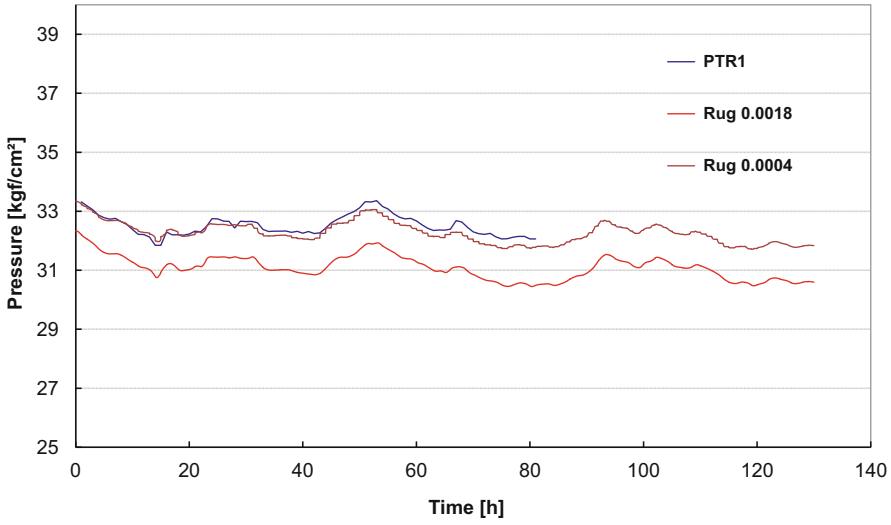

Fig. 14 Adjusted pressure trend at delivery point 13

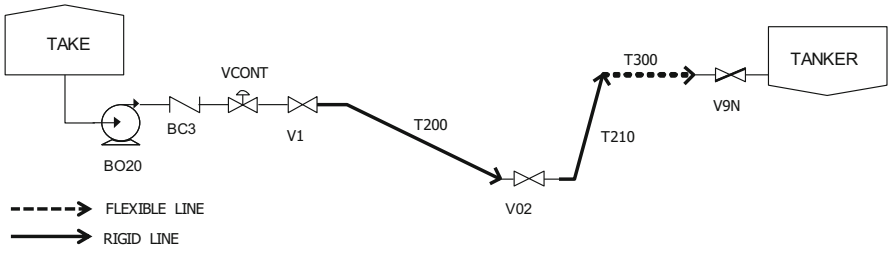

Fig. 15 Fast Transient Sample Model (Schematic)

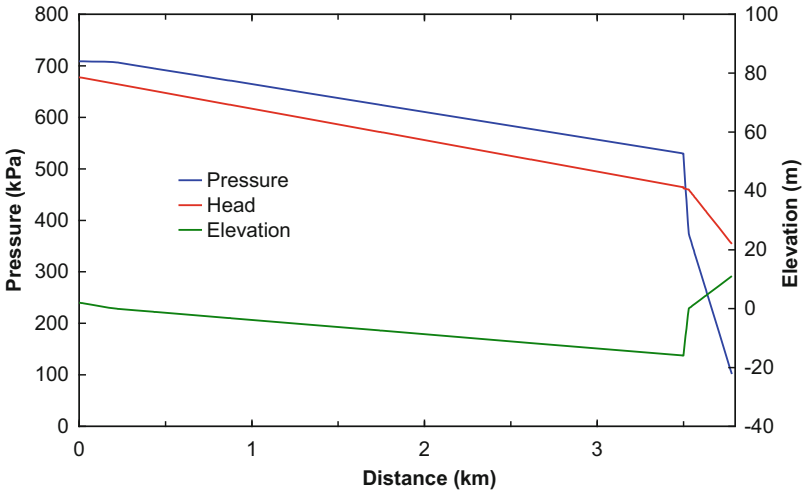

Fig. 16 Pressure, head, and elevation profiles at steady state

bulk modulus of 1.381 GPa. All the properties were taken at 65 °C, a typical operational temperature.

The scenario modeled is characterized by the closing of the tanker valve (V9N), with the pipeline operating at steady state as initial condition, as presented in Fig. 16. As the tanker valve closes, the flow rate is reduced causing a pressure raise that can be estimated by Joukowsky's equation. The information of flow reduction and pressure increase travels through the pipeline at acoustic speed. In response to the flow reduction, the pump discharge pressure increases according to its characteristic curve. The control valve starts to open, in an attempt to return the flow rate to the adjusted setpoint. When the surge pressure becomes greater than the maximum pump discharge pressure (shut-off value), the pressure gradient prevailing in the line tends to produce reverse flow. At this moment, the check valve starts to close and, depending on its response time, some relief of the pressure can occur due to a pump reverse flow. When the check valve closes, another pressure pulse is induced in the opposite direction. As a result, the pressurized pipeline is closed at both ends, with a pressure wave traveling between the extremities, which is gradually damped. Since the surge pressure is observed in seconds, the heat exchange between the fluid and the environment was not considered once it involves larger periods of time. So, an isothermal model is a usual hypothesis to perform this analysis.

Influence of the Valve Closing Times

Considering the scenario modeled, the tanker valve (V9N) with smaller closing time produced higher pressure surge, for the same operating conditions, once the closing time is directly related to the deceleration of the fluid flow (Propson 1970). To analyze this parameter, the block valve was modeled with different closing times: 1 s, 30 s, 60 s, and 90 s. The transients were generated when the motorized block valve V9N, located at the tanker, was closed. It can be observed in Fig. 17a that

shorter closure times, which are normally used in valves for leakage prevention, will produce overpressures significantly greater than the normal operational pressure. In field operations, it is possible to increase the valve closing time in order to minimize the over pressure produced. However, the increase in valve closing time is limited by the primary purpose of this block valve. Closing times of the order of the pipe period ($2\,L/v_a$) can be considered as instantaneous closure. This condition is verified for $t =$ 1 s. According to the Joukowsky's equation, for $\Delta u = 4.4$ m/s, $\rho = 943$ kg/m^3, and v_a = 1237 m/s, the calculated surge pressure is $\Delta P = 5.13$ MPa (52.3 kgf/cm^2) at the downstream valve (V9N), almost the same value observed in Fig. 17a (5190 kPa or 53.0 kgf/cm^2).

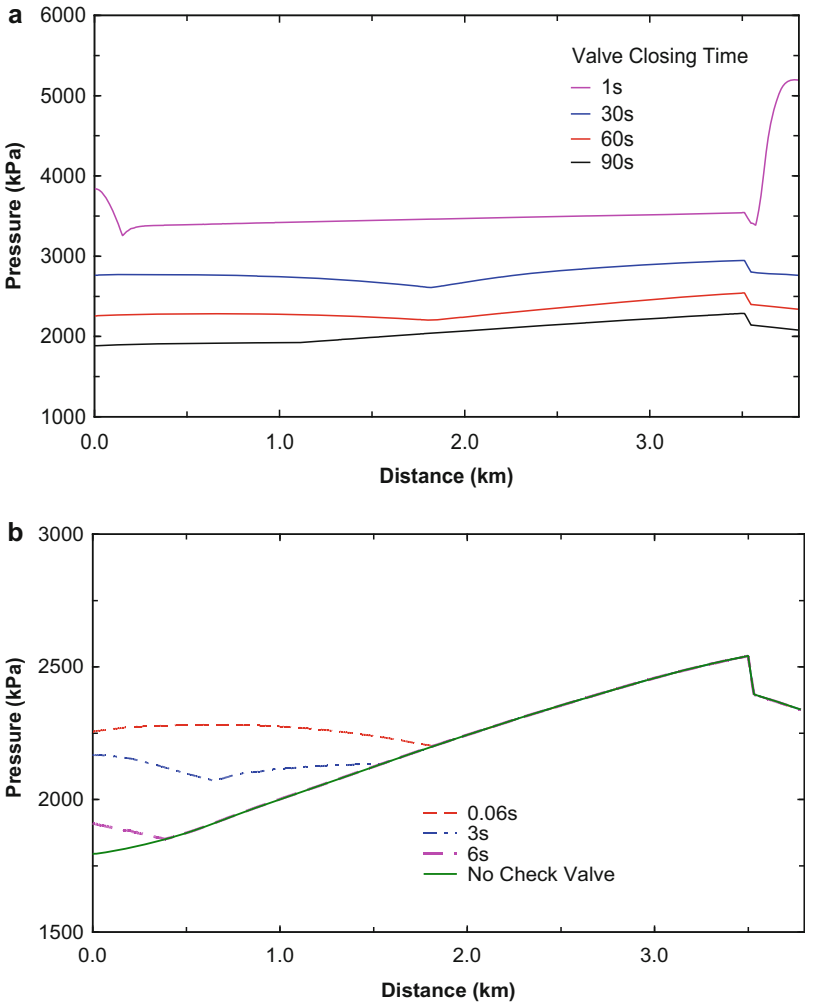

Fig. 17 Valve influence in maximum pressure profile along the pipeline. (**a**) Influence of block valve closing times. (**b**) Influence of check valve closing time

However, for greater closing times, the reflected pressure wave returns to the motorized valve, which is still partially opened, and produces a significant reduction of the maximum pressure in the valve and along the pipeline, since part of the pressure surge is relieved by the flow through the valve.

The final maximum pressure profile is also a function of the transient response of other equipaments, besides the closing valve. An example is a check valve, which is usually installed at pump discharge. Check valves are used to prevent backflow when the pump is turned off and to prevent the pressure waves cruising in the reverse flow direction jeopardizing the integrity of the equipment. Characteristic closing times for check valves are between 0.01 and 0.1 s. Figure 17b resents the maximum pressure distribution along the pipeline, obtained with different check valve response times. It can be seen in the figure that the maximum pressure profile presents an inflection near midpoint, due to the closing of the check valve, and because of its fast response, another water hammer effect is generated, increasing the pressure at this end of the pipeline. However, for closure times greater than 6 s (corresponding to a malfunctioning valve), the system responds as if the check valve was not present, thereby allowing for a total flow reversal through the pump.

Influence of the Valve Discharge Coefficient Curve

The discharge coefficient curve represents the dependence of the valve discharge coefficient with the stem position, and determines the way the flow rate through the valve varies with the opening fraction. The characteristic curves used in this topic are presented in Fig. 18a. Typically, gate valves produce significant flow variation only when they are almost closed. On the other hand, ball and butterfly valves produce a more gradual variation of the flow rate during the closure period. As a result, the more significant flow deceleration produced by the gate valve generates pressures that are greater than the ones given by the closure of a butterfly or a ball valve. Works for determining the ideal procedure for valve closing that produce the smaller pressure rise have been developed by many authors, like Streeter (1963) and Azoury et al. (1986). The results presented in Fig. 18b characterize the different behaviors of the valves, where all closing times were equal to 60 s.

Influence of the Pump Curve and Shut-off

The influence of the discharge pressure at zero flow rate (stagnation pressure or shut-off head) can be observed considering different pump curves, operating at the same point (0.222 m^3/s or 800 m^3/h), as shown in Fig. 19a. It can be noticed in the figure that when the pressure wave arrives at the pump, it induces a reduction of the flow and, as consequence, a modification of the discharge pressure, dictated by the pump curve. When the flow rate reaches zero, the discharge pressure is kept constant and the maximum pressure at this point is the sum of the maximum discharge pressure with the value produced by the pressure pulse. As a consequence, pumps with lower shut-off values produce lower surge pressures, as illustrated in the results presented in Fig. 19b.

Influence of Pipeline Flexibility (Elasticity Modulus)

The acoustic wave speed, v_a, is a function of thermodynamic fluid properties (compressibility modulus, K, and density, ρ) and pipe properties (diameter, D,

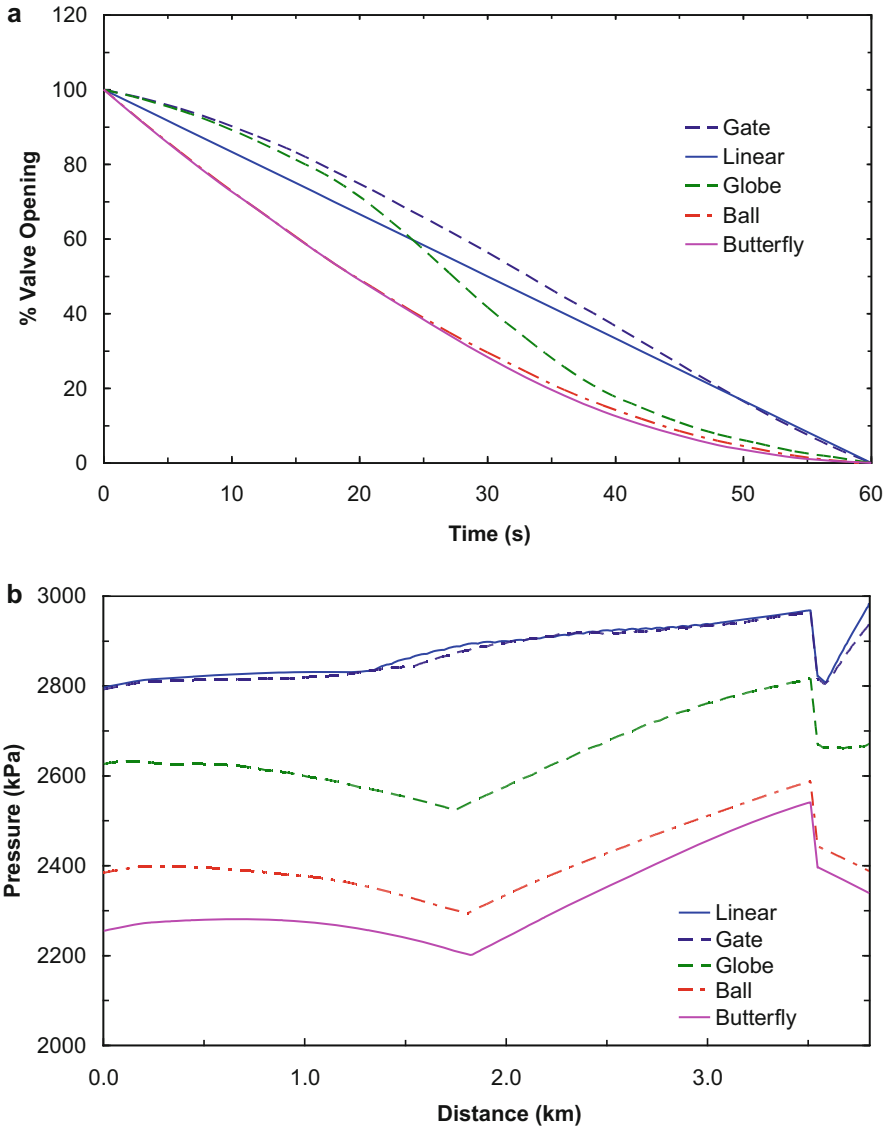

Fig. 18 Impact of valve discharge coefficient. (**a**) Closure curve of the block valve V9N. (**b**) Maximum pressure profile for different valve curves

thickness, e, and elasticity modulus, E) as defined in Eq. (53). Flexible pipes are composed by layers of distinct materials such as, steel, polymers, rubber, etc. From manufacturer's data, it can be verified that the acoustic speed in flexible pipes can experience a reduction of the order of 2/3 of the speed prevailing in a rigid pipeline. All calculation performed so far have assumed that the elasticity modulus of the

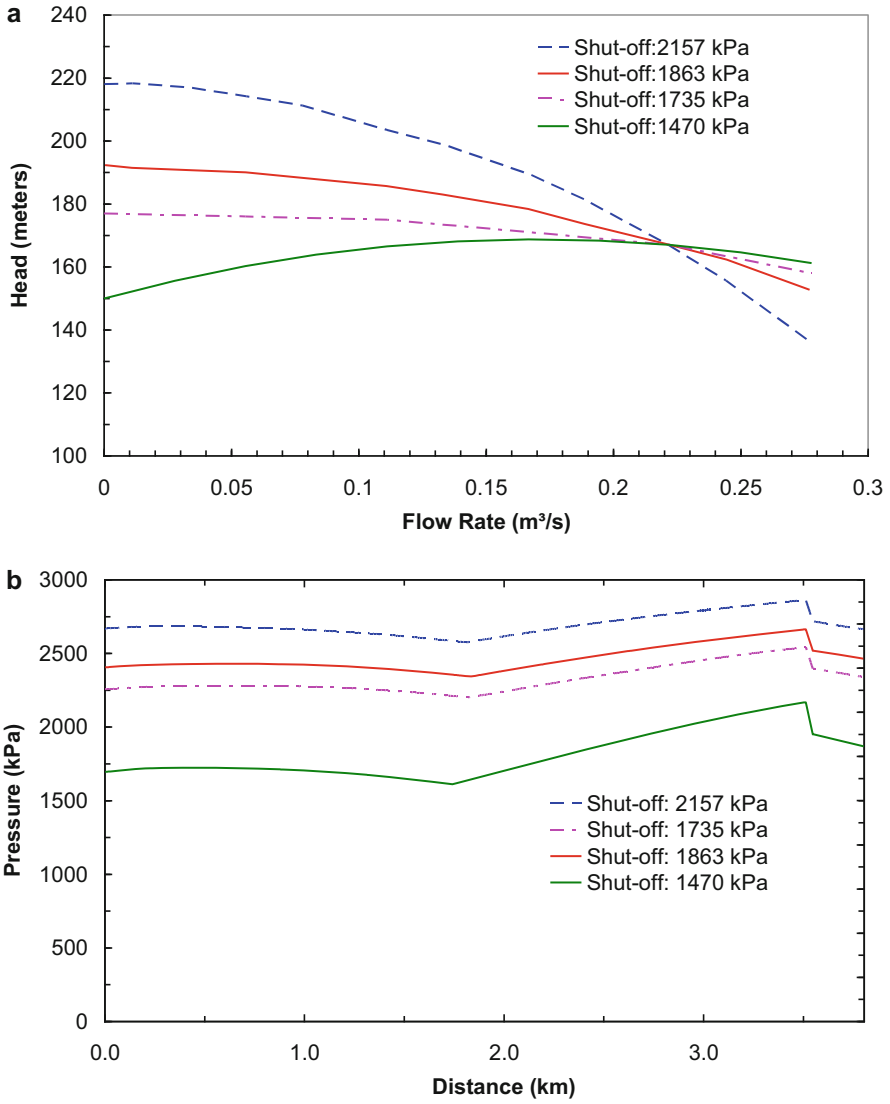

Fig. 19 Modified pump curves. (**a**) Different pump curves with the same operation point. (**b**) Influence of shut-off value in maximum pressure

flexible pipe was equal to that of the rigid steel pipe. For closing times of the block valve (V9N), of the order of 60 s, the variation of the modulus of elasticity of the flexible line does not change the profiles of maximum pressure. However, for an instantaneous valve closing, about 1 s, it is verified that the maximum pressure at the block valve V9N experiences a reduction of 11.33 kPa (10 kgf/cm^2), when compared

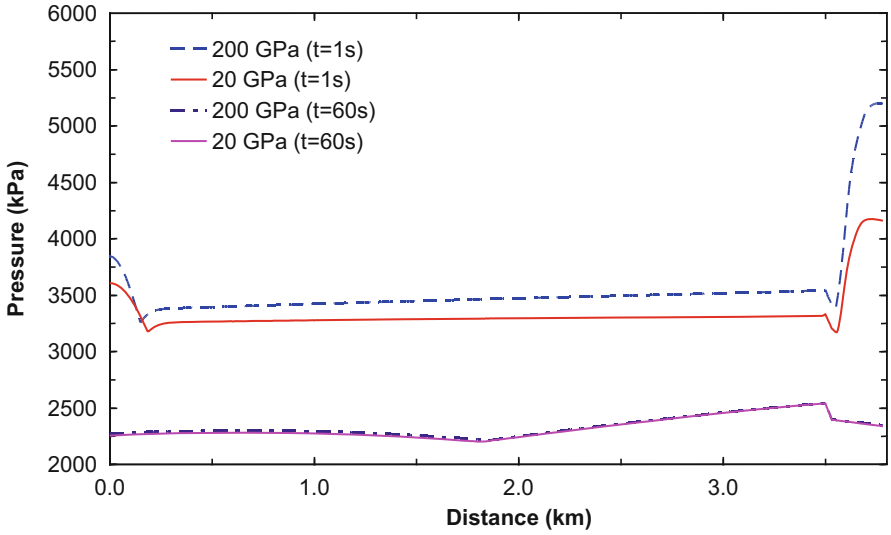

Fig. 20 Influence of flexible pipe modulus of elasticity on maximum pressure profile

with the case in which the modulus of elasticity of the flexible pipe is assumed to be equal to that of a steel rigid pipe. Figure 20 shows these results.

Thermal Transient Aspects: Liquid Phase Sample Model

Depending on the type of the problem, the hydraulic simulation can be performed considering an isothermal situation (as in the case of fast transients in liquids) and in others the temperature variation directly interferes in the analyzed situation. Due to the oil and derivatives production characteristics, these products can enter the pipeline system at temperatures above the environmental temperature. Typically, for marine fuel oil, it must be warmed up, to reach a lower viscosity in order to flow more easily. So, to define the operating pipeline conditions, the influence of the temperature on the flow must be especially evaluated. On the other hand, when the focus is the operational security, the highest and lowest fluid temperatures must be observed. The minimum temperature must be a restriction given the limit for the fluid's fluidity point (pour point), which, if reached, may cause a pipeline blockage. The maximum temperature is limited by the pipeline's mechanical design temperature. To fulfill the analysis of a specific case, additional input data, as products and material thermal properties, are needed to configure the computational model. Frequently, these data come with high uncertainty. Furthermore, the nonlinear nature of the problem can amplify the uncertainty levels of the input variables on the results, therefore, when analyzing the results, care should be taken with the level of reliability of the model output.

Table 3 Thermal properties for pipe, coating, and soil

Layer (Material)	Thermal Conductivity [W/(m K)]	Heat Capacity Cp [J/(kg K)]
Pipe (steel)	60.500	444.0
Thermal insulation (PU)	0.038	1.04
Coating (PEAD)	0.450	2.25
Soil	1.616	3.23

Several transport systems employ buried pipelines. In these situations, the thermal capacitance of the system can be very high, and thermal equilibrium (hydraulic and thermal steady state) can take a long time to be achieved, reaching the order of days. Thus, the simulation analyst must be very careful with the type of response that one intends to obtain, especially when dealing with a transient analysis. As an example, some results will be presented for a 99 km pipeline, 16″ nominal diameter, 8.3 mm polyurethane coating, and 2″ thick polyurethane thermal insulation. The thermal properties of the materials for all layers are shown in Table 3.

The calculated temperature profile in steady state is shown in Fig. 21a. The values used represent the design condition. At the same figure, the field temperature at 100 km is included. A significant difference between the prediction and field data can be seen. However, the pipeline has been in operation for more than 20 years, and it is difficult to determine the variation of a specific property due to material degradation. Typically, thermal insulation ages, resulting in large uncertainty in the insulation thermal conductivity due to its degradation in the presence of water. The large temperature unconformity indicates that the insulation is far degraded, and the design data is no longer valid. The insulation thermal conductivity and the soil temperature are then gradually adjusted in order that the calculated fluid temperature at the pipeline exit and the field data match.

The previously presented case represents a steady state situation, corresponding to a pipeline operating with a product at 25 °C (with the ground at 20 °C). However, when another batch is introduced in the pipeline. With another product at 85 °C, a transient regime is observed where variations in flow and temperature occur, as shown in Fig. 21b. After 6 days, the product arrival temperature is approximately constant, but a small variation of the ground and pipe wall temperature is still observed, indicating that the steady state temperature has not yet been reached.

PIG Operations

Pigging is a common practice in the petroleum and natural gas industry. In general terms, a PIG is a solid plug that is introduced into the pipeline to be serviced. Fluid is pumped upstream of the PIG to provide the necessary force to set the device in motion, and to perform the desired task, that is, removing deposits from the pipe wall, removing water (or other fluid) from the pipeline, or driving an inspection tool (see ▶ "Flow Assurance in Pipelines"). The use of PIGs has become a standard industry procedure. A great variety of PIG models is available for each particular

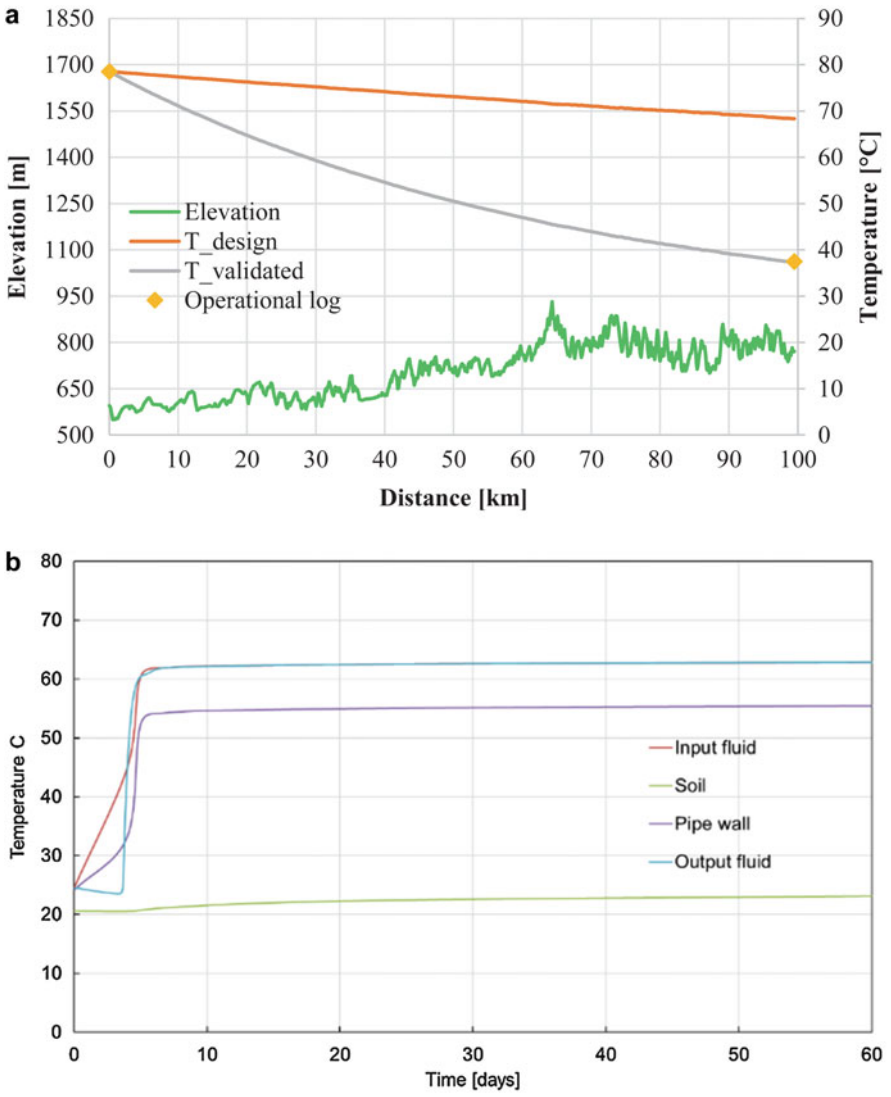

Fig. 21 Temperature profile. (**a**) Steady state temperature profile along pipeline. (**b**) Transient temperature evolution

application. A difficulty often faced by the engineer when designing a pigging operation is the lack of reliable tools for the prediction of the many variables related to the motion of the PIG through the pipeline. Most of the available knowledge is based on field experience. Hence, there is often some guesswork and, consequently, a degree of uncertainty in selecting the best PIG by estimating its speed, the required driving pressure, and the amount of backward/forward bypass of fluid.

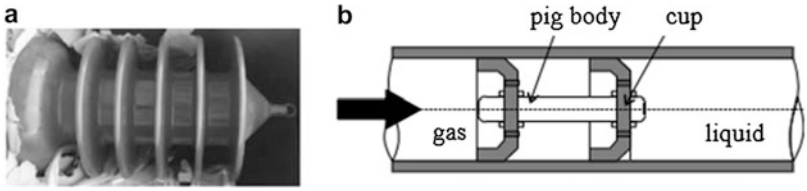

Fig. 22 Sealing PIG (Tolmasquim and Nieckele 2008). (**a**) Typical sealing PIG. (**b**) Schematic view of a sealing PIG inside a pipeline

The PIG velocity is directly related to the sealing efficiency of the PIG, and requires that the flow rate be maintained within certain limits. The flow rate and the pressure distribution depend directly on the pipeline topography and phases distribution. Even for single phase models, while gas flows in one section of the pipeline, liquid can be flowing in another section. Therefore, the operational design should also account for the pressure distribution along the pipeline, in order to guarantee the level of operating pressure in the pipeline, avoiding the occurrence of either slack flow or excess pressure.

A typical sealing PIG is formed by piston-type cups attached to a cylindrical body (Fig. 22a). In order to produce efficient sealing, PIGs have nominal diameters larger than the pipe diameter. Figure 22b is a sketch of a sealing operation. Fluid pumped upstream of the PIG provides the necessary pressure difference to overcome the contact force at the wall, to displace the fluid downstream of the PIG, and to accelerate the PIG.

To determine the PIG displacement, the following force balance equation must be solved coupled with the flow conservation equations:

$$m_{\text{pig}} \frac{dV_{\text{pig}}}{dt} = (P_1 - P_2)A - m_{\text{pig}}\, g \sin\theta - F_{\text{at}}\left(V_{\text{pig}}\right); V_{\text{pig}} = \frac{dx_{\text{pig}}}{dt} \qquad (54)$$

where x_{pig} and V_{pig} are the PIG position and velocity, and m_{pig} is its mass. P_1 and P_2 are the upstream and downstream pressures at the PIG's face. F_{at} is its contact force, and it can have different values depending if the PIG is moving (dynamic contact force, F_{dyn}) or in eminence to move (static contact force, F_{st}). The dynamic and static PIG contact force can have different values depending on the direction of the PIG's movement. F_{dyn} can also be proportional to its own velocity.

In the next sub-section, an example of a pigging operation is presented.

Liquid Displacement Operation in Oil Pipeline

To illustrate an example of PIG operation, a liquid displacement operation in oil pipeline is described. This operation might be needed, for example, if the pipeline needs repair, thus, for safety reasons, nitrogen (inert gas) must be introduced into the pipeline. For the operation, there are several issues that must be controlled. The volume of nitrogen must be minimal to reduce costs, the PIG must not travel at high speed, not only because it is dangerous, but to guarantee that all oil is removed. The

pressure inside the pipeline cannot be too small, to avoid column opening (liquid vaporization), and it cannot also be too high, since the pressure inside the pipeline must be below the maximum allowable operating pressure (MAOP), to avoid rupture of the pipeline.

Let us consider a pipeline with 117 km in length between a pipeline terminal and a refinery, with an intermediate pumping station at 60 km, as shown in Fig. 23a. Due to the steep slope, after km 52, the pipeline thickness is enlarged, to allow for higher pressure (MAOP). The pipeline characteristics are: steel, nominal diameter 30 in (762 mm), with wall thickness e varying from 9.53 mm (from 0 to 53,8 km) to 14.3 mm for the remaining pipeline.

It is desired to remove the oil from the pipeline. To this end, nitrogen is injected, with a 50 kg separator flexpig. Owing to the pipeline profile (Fig. 23a), the oil

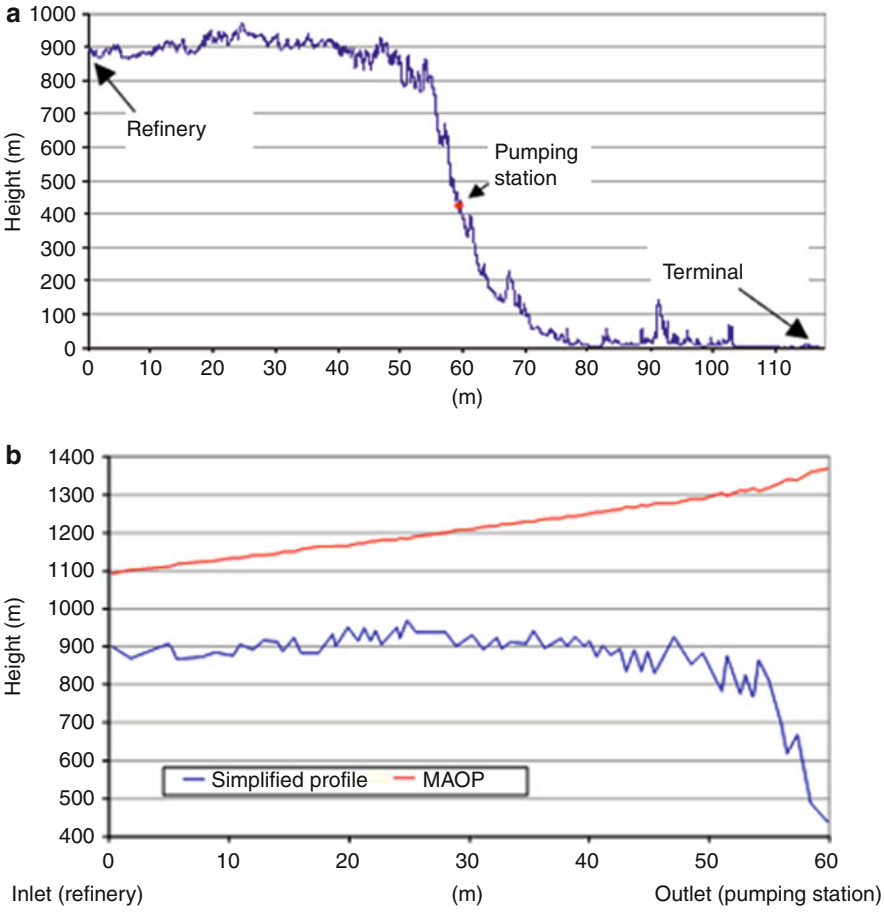

Fig. 23 Pipeline profile. (**a**) Actual pipeline profile. (**b**) Simplified section profile and maximum allowable operation pressure

displacement was from the refinery to terminal, that is, in the opposite direction to the normal operational direction. The pipeline profile has a great influence on PIG passage operations involving liquid and gas. In order to reduce the computational effort, the elevation profile was simplified, but keeping a representative number of points as shown in Fig. 23b. The maximum allowable operating pressure (MAOP), also illustrated in Fig. 23b, is represented in meters of liquid column in order to facilitate its visualization in relation to the pipeline elevation profile.

Liquid nitrogen was stored in a low-pressure cryogenic cylinder. Leaving the cylinder, the nitrogen pressure was raised to the desired level; it was vaporized and then injected into the pipeline. The nitrogen properties were: $W = 28$ kmol/kg, $Z = 1.04$, and $\mu = 0.015$ cP. The oil properties were: $\rho = 828$ kg/m^3, $a = 1218$ m/s, and $\mu = 2.6$ cP. The PIG contact forces (static and dynamic) were equal and the same in both directions, but they varied with the pipe wall thickness from 85 kN to 83 kN.

In this operation, nitrogen flow was imposed at the entrance at 5 kg/s and the liquid flow was controlled by a valve at the pipe exit (Eq. 36). The product of the valve discharge coefficient and its opening is given by $(C_V A_v) = (C_V A_v)_o \chi$, where $(C_V A_v)_o = 0.005$ m^2 corresponds to the valve completely opened, and χ is the percentage of valve opening and downstream pressure = 1 atm. The exit valve opens slowly to control the initial PIG velocity, taking 1 minute to be 60%. This aperture is kept constant in order to prevent the PIG velocity from exceeding a desired threshold value (0.7 m/s), with small variations being acceptable. It is desirable to maintain the flow with the column full, and strong restrictions regarding minimum pressure ($P_{\min} = 2$ atm) must be imposed. Finally, the maximum allowable pressure cannot be exceeded. The point of highest altitude is the critical point, as the pressure drops, and column opening may occur.

Figure 24a shows the oil hydrostatic pressure distribution along the pipeline at time equal zero. The MAOP is also shown, which is, as desired, above the inner pressure. According to ASME B.31.4 (2004), the MAOP is allowed to be exceeded by 10% for a short period of time, or stretch of pipeline, with the same thickness and material, but it is recommended to analyze different operation strategies that avoid

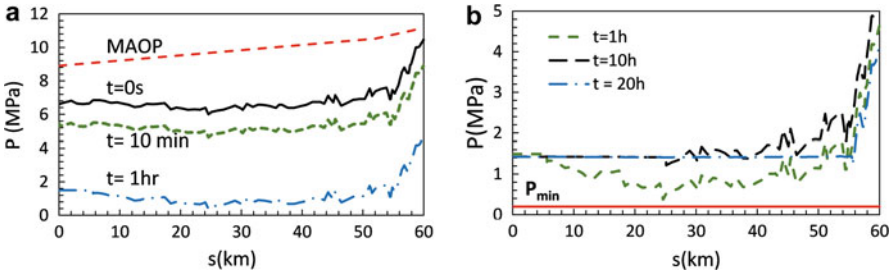

Fig. 24 Pressure distribution. (**a**) Pressure at initial time instants and MAOP. (**b**) Pressure at advanced time instants and minimum allowed pressure

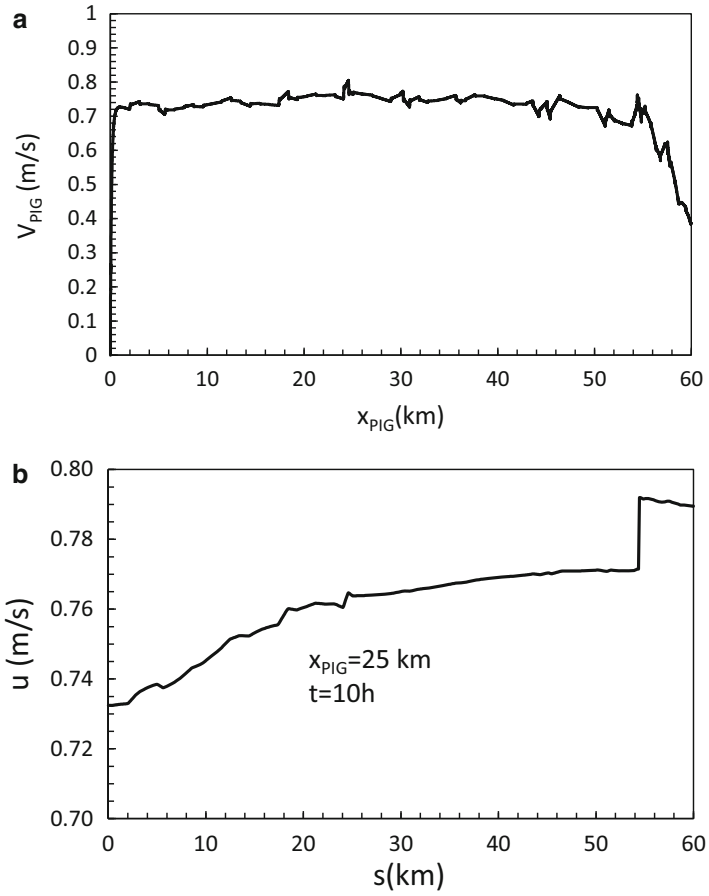

Fig. 25 PIG velocity and oil velocity. (**a**) PIG velocity as a function of its position. (**b**) Nitrogen and oil velocity along the pipeline. $t = 10$ h

the occurrence of pressure peaks, such as, for example, the reduction of nitrogen flow or a slower increase in the flow at the beginning of the operation.

As the exit valve is opened, discharging to ambient pressure, and nitrogen is introduced in pipeline, the overall pressure drops significantly. Figure 24b shows the pressure variation along the pipeline at advanced time instants after the beginning of the operation, showing values above the minimum pressure to avoid column opening, which is also included in the figure. Since gas is much lighter than liquid, the pressure drop at the region filled by nitrogen is very small, and by the small pressure drop region, the PIG displacement along the pipeline can be clearly seen.

Figure 25a shows that the configuration designed for the operation was also successful in relation to the pig's velocity. Finally, Fig. 25b shows the fluid velocity

along the pipeline after 10 h of the beginning of the operation. The PIG position is indicted in the figure, thus, velocities upstream of its position correspond to the nitrogen and downstream to the oil. Since the density of the oil is approximately constant, its velocity is almost constant. At 52 km, one can observed larger oil velocity, due to the reduction on the pipeline cross-section area.

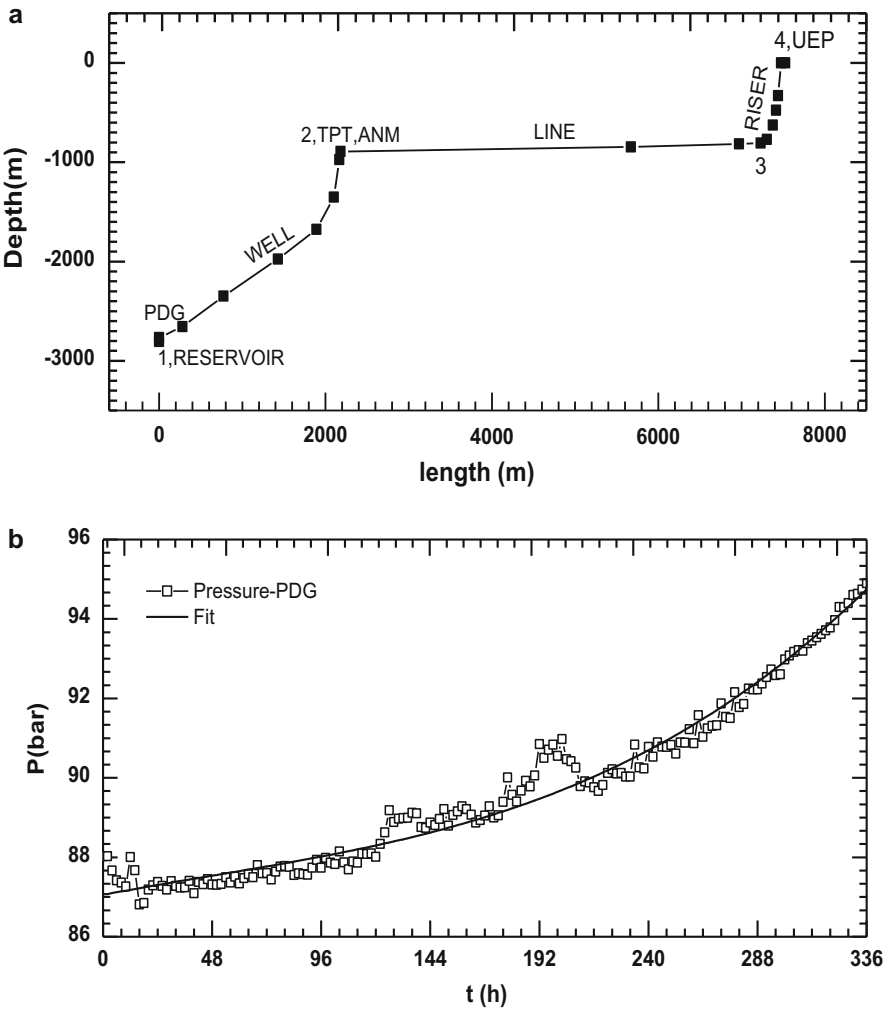

Fig. 26 Pipeline configuration and boundary condition. Cruz (2011). (**a**) Production well geometry. (**b**) Inlet well pressure

Multiphase Wax Deposition

Wax deposition is critical in offshore deep-water production facilities where the flowlines are exposed to the cold ocean temperatures that prevail at elevated water depths. The warm oil exiting at approximately 60 °C from the well head loses heat to the surrounding environment at, typically, 4 °C as it flows to the production platforms. If the crude oil temperature falls below the wax appearance temperature (WAT), the wax may precipitate and deposit along the inner walls of the pipeline. Deposition of heavy paraffin molecules in the inner walls of pipelines is a serious problem for the petroleum industry due to the potential capital losses that it imposes to the operators. Indeed, paraffin deposition may lead to loss of production, increased pumping power, elevated remediation costs, and even loss of pipelines due to its total blockage (see ▶ "Flow Assurance in Pipelines").

This example illustrates the determination of wax deposition in a producing well, shown in Fig. 26a. At the reservoir, there is a pressure downhole gauge (PDG), and at the Christmas tree (ANM) and production unit (UEP) there are temperature and pressure transducers (TPT). Due to the wax deposition, the pressure necessary to maintain a given flow rate increases, since there is a restriction of the pipe cross-section area.

The fluid in the reservoir has RGO = 100 m^3/m^3, 1% of water fraction, and WAT equal to 18 °C. The oil and water density were determined based on the black-oil model (Beggs and Brill 1984). The gas specific gravity was 0.7. The solubility curve was adjusted to fit the field data. The inlet pressure at the well was adjusted as a function of time from the well data (Fig. 26b).

The growth of the deposited layer was accounted for by a molecular diffusion mechanism, as suggested by Burger et al. (1981). The wax deposit mass is $m_{\text{wax}} = \rho_{\text{wax}}(1 - \varphi)\, A_d\, ds$, where $A_d = A - \pi r_d^2$, is the cross-section deposit area (r_d the deposit radius), ρ_{wax} the solid wax density, and φ is the deposit porosity. In this model, the deposition only occurs when $T_{\text{int}} <$ WAT and the wax diffusion flux toward the cold wall is estimated by Fick's law of diffusion

Table 4 Drift flux parameters

	V_{drift}	C_o
Slug vertical	$0.35\left(g\,D\,\frac{\rho_L-\rho_G}{\rho_L}\right)^{1/2}$	1.2
Slug horizontal or inclined	$Fr \le 3.5$ $\sqrt{g\,D}(0.35\cos\theta + 0.54)$ $Fr > 3.5$ $0.35\sqrt{g\,D}\cos\theta$	$Fr \le 3.5$ $1.05 + 0.15\sin^2\theta$ $Fr > 3.5$ 1.2
Stratified		
Bubble vertical	$1.53\left[g\sigma(\rho_L - \rho_G)\rho_L^2\right]^{1/4}$	1.2

Table 5 Internal heat transfer coefficient

	h_i/h_L	$Nu_L = h_L\, D/k_L$
Slug vertical	$(\alpha_L)^{-0.9}$	$0.023\ Re_{sL}^{0.8} Pr_L^{0.33}$
Slug horizontal or inclined	$\frac{k_L}{k_m}$	$125\left(\frac{u_{sG}}{u_{sL}}\right)^{\frac{1}{8}}\left(\frac{\mu_G}{\mu_L}\right)^{0.6} Re_{sL}^{\frac{1}{4}} Pr_L^{\frac{1}{3}}$
Stratified	$\frac{k_L}{k_m}$	$0.023\ Re_{sL}^{0.8} Pr_L^{0.33}$
Bubble vertical	$(\alpha_L)^{-0.83}$	$0.0155\ Re_{sL}^{0.83} Pr_L^{0.5}$

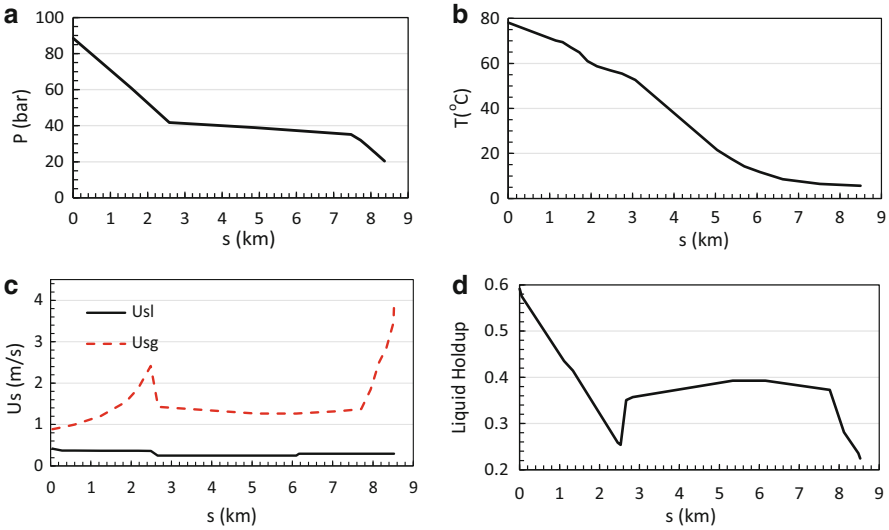

Fig. 27 Pressure, temperature, superficial velocity, and holdup distribution along the line after 1 h. (**a**) Pressure. (**b**) Temperature. (**c**) Superficial velocity. (**d**) Holdup

$$\frac{\partial\, m_{\text{wax}}}{\partial\, t} = -\rho_m\, D_{\text{wax}}\, (2\,\pi\, r_d\, dx)\ \left.\frac{\partial\omega}{\partial r}\right)_d ;\ \left.\frac{\partial\omega}{\partial r}\right)_d = \left.\frac{\partial\omega}{\partial T}\,\frac{\partial T}{\partial r}\right)_d$$
$$= \frac{\partial\omega}{\partial T}\ \frac{U_G(T - T_\infty)}{k_m} \tag{55}$$

where D_{wax} is the molecular diffusion coefficient of the liquid wax in the solvent oil, ω is the concentration or volume fraction of wax in the solution, $\partial\omega/\partial T$ is the solubility curve, and the subscrit d indicates the deposit interface.

To solve the problem, the drift model was selected. Table 4 shows V_{drift} and C_o drift flux parameters, while Table 5 presents the internal heat transfer coefficient, for each flow pattern (Beggs and Brill 1984). In both tables, the governing parameters are: Froud number $\text{Fr} = j/\sqrt{g\,D}$, Prandtl number $\text{Pr}_L = \mu_L cp_L/k_L$, and superficial Reynolds number $\text{Re}_{\text{sL}} = \rho_L|u_{\text{sL}}|D/\mu_L$.

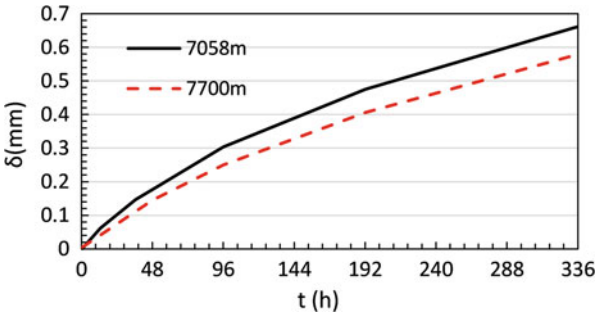

Fig. 28 Time evolution of deposit thickness at $s =$ 7058 m and $s = 7700$ m

Figure 27 presents the axial distribution of pressure, temperature, superficial velocities, and holdup after 1 hour of the beginning of the deposition. A strong pressure drop can be seen as the fluid travels from the reservoir to the Christmas tree, not only because of the head loss along the pipe, but mainly due to reduced depth. Between the Christmas tree and the riser, the pressure drop is small, since the pipe is nearly horizontal. Finally, another strong pressure drop is observed at the riser. The temperature falls continuously along the pipe. In the first stage, the temperature drop is associated with the pressure drop and dissociation of gas. Between the Christmas tree and the riser, the temperature drop is primarily due to heat exchange with the cold marine environment. In the final pipe segment, the temperature is almost constant, since it is very close to the external environment temperature. The distributions of the liquid and gas superficial velocities present a direct correlation with the liquid holdup distribution. At the first and last pipeline, where there is a decrease in the line depth, an increase of gas superficial velocity due to gas dissociation from oil can be seen. At the Christmas tree, there is an increase in liquid holdup due to water injection, which causes a decrease in superficial velocities of gas and liquid. Along the horizontal line, both liquid holdup and superficial velocities are approximately constant.

Figure 28 illustrates the time evolution of the deposit thickness in two positions in the horizontal line, near the base of the riser ($s = 7058$ and $s = 7700$ m). A faster growth can be seen in the beginning of the process. Qualitatively the behavior is the same in both positions.

Final Remarks

At the present chapter, a brief review of the mathematical and numerical modeling necessary to determine the flow variables along pipelines was presented, followed by special care that must be taken to build the desired models. Finally, a few examples were presented to illustrate typical results.

Numerical simulation of pipeline flow is a useful tool during design and operation of pipelines. However, care must be taken not only to select the appropriate software

but also to analyze the data obtained. Before starting a numerical analysis, the user must clearly define the main results it is being search. To this end, hypothesis for the desired analysis must be well stated, since the software selection depends on that. Another very important step is to guarantee that numerical parameters do not affect the flow prediction, meaning that mesh distribution and time step definition, combined with the discretization schemes employed do not alter the final results obtained. So, a user must always investigate the impact of these parameters on its solution. Finally, a critical analysis of the results must be realized.

References

ASME B31.4-2002 (2004) Pipeline transportation systems for liquid hydrocarbons and other liquids. Revision of ASME B31.4-1998. New York

Azoury PH, Baasiri M, Najm H (1986) Effect of valve-closure schedule on water hammer. J Hydraul Eng 112(10):890–903

Beggs DH, Brill PJ (1984) Two-phase flow in pipes. University of Tulsa, Tulsa, Oklahoma

Bird RB, Stewart WE, Lightfoot EN, Klingenberg DJ (2015) Introductory transport phenomena. Wiley

Brennen C (2005) Fundamentals of multiphase flow. Cambridge University Press, Inc, Pasadena

Burger E, Perkins T, Striegler J (1981) Studies of wax deposition in the Trans Alaska pipeline. J Pet Technol:1075–1086

Cruz SR (2011) Wax deposition study in a multiphase pipe flow. In Portuguese. Master Dissertation, Mechanical Engineering Department, PUC-Rio. Rio de Janeiro, Brazil. https://doi.org/10.17771/PUCRio.acad.24985

Hasan R, Kabir S (2018) Fluid flow and heat transfer in wellbores, Textbook series, 2nd edn. Society of Petroleum Engineers, Texas

Holman JP (2010) Heat transfer, 10th edn. McGraw Hill, Boston

Incropera FP, Dewitt DP, Bergman TL, Lavine AS (2007) Fundamentals of heat and mass transfer, 6th edn. John Wiley and Sons

Ishii M, Hibiki T (2006) Thermo-fluid dynamics of two-phase flow. Springer-Verlag

Lagoni P, Barley J (2007) On simulation accuracy, pipeline simulation interest group, PSIG 0711, Calgary, Canada

Michelsen ML, Mollerup JM (2007) Thermodynamic models: fundamentals and computational aspects, 2nd edn. Tie-Line Publications, Holte

Poling BE, Prausnitz JM, O'Connell JP (2001) The properties of gases and liquids, 5th edn. McGraw Hill

Pritchard PJ, Mitchell JW (2015) Fox and McDonald's introduction to fluid mechanic, 9th edn. John Wiley and Sons

Propson TP (1970) Valve stroking to control transient flows in liquid piping systems, University of Michigan, PhD thesis

Streeter VL (1963) Valve stroking to control Waterhammer. Journal of Hydraulic Division, ASCE 89(2):39–66

Swamee PK (1993) Design of a submarine oil pipeline. J Transp Eng 119(1):159–170

Tolmasquim ST, Nieckele AO (2008) Design and control of pig operations through pipeline. J Pet Sci Eng 62:102–110

Val Matic White Papers (2018) Surge control in pumping systems

Wylie EB, Streeter VL (1978) Fluid transients. McGraw Hill